J KAU: Earth Sci., **vol. 4**, pp. 67-103 (1411 A.H./1991 A.D.)

Application of Geophysical Techniques to the Interpretation of Aeromagnetic Survey Data, South Eastern Desert, Egypt

AHMED A. AMMAR and SAID I. RABIE
Nuclear Materials Authority, Maadi, Cairo, Egypt

ABSTRACT. The regional-structural framework of an area (Gabal Um Samiuki) located in the South Eastern Desert of Egypt, was delineated through the integraiton of six modern geophysical techiques from the informations and interpretations of aeromagnetic survey data reduced to the north magnetic pole (RTP).

Two main average interfaces at depth 0.8 and 2.0 kms below the measuring level were calculated through the application of local power spectrum. Filtering combined with the analytical downward continuation of the RTP magnetic data at the assigned two interfaces was conducted. Four maps were drawn, two at each interface: one for the regional, and the other for residual components of the magnetic field. In addition, the magnitude of the normalized total vector (gradient) of the field intensity was calculated at the two stated interfaces and two more maps were constructed. Moreover, variations of the phase angle were calculated, and two other maps were prepared. Techniques of statistical analysis of trends using the overlap method were conducted for most of the resulting maps and ten frequency curves were plotted.

Results from this study suggest the existence of five major magnetic-structural trends namely: Gulf of Suez-Red Sea (NNW and NW), Najd (WNW), Tethyan (E-W), Syrian arc or Qattara (ENE) and Trans-African (NE). The meridional (N-S) and Gulf of Aqaba (NNE) trends are not represented in the study area. The preferred major trends of the whole lineaments coincide with the mentioned five directions. There are series of uplifted and subsided blocks (or folding in the form of anticlines and synclines) correlate well with three main trends: WNW, E-W and ENE. The Najd and Syrian arc trends are proved to be similar in many aspects and are considered as conjugate trends. The deep-seated tectonic zones (diabase dykes) are associated with the NW trend, into one of which lies Gabal (G.) El Kahfa ring complex. A similar feature to G. El Kahfa was discovered at depth within the same zone of magnetic highs.

Introduction

The study area is located in the South Eastern Desert of Egypt (Fig. 1), and covers a surface area of about 7000 square kilometers. Topographically, the most conspicuous feature of the study area is the rugged, highly-dissected Precambrian terrain of the Red Sea hills, that runs approximately parallel to the coast, forming a series of mountain groups as opposed to one continous range.

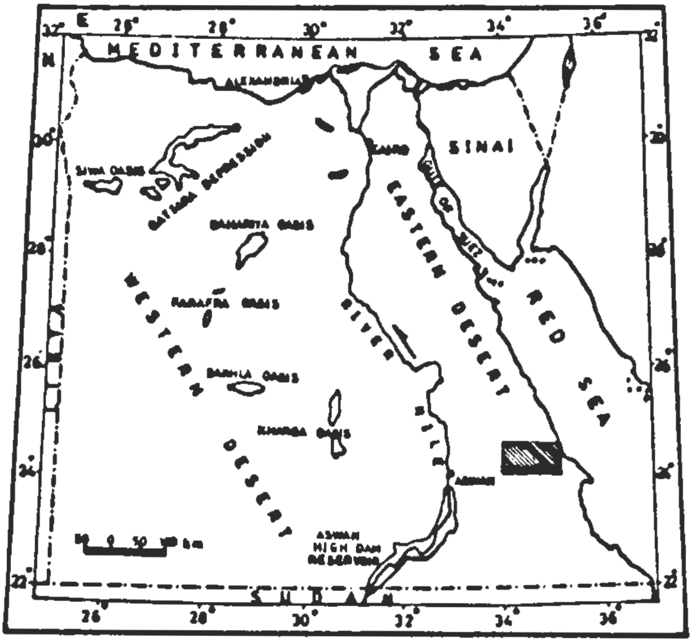

FIG. 1. Map of Egypt showing the location of Um Samiuki area, South Eastern Desert.

The area under consideration was mapped from the air by magnetic and radiometric methods as a part of the complex project of Assessment of the Mineral Potential of the Aswan Region. It was organized in co-operation with the United Nations Development Programme and the Geological Survey of Egypt, in the South Eastern Desert of Egypt.

The aerial (magnetic and radiometric) survey was carried out along parallel flight lines nearly oriented N60°E to cross the regional sturctural trends in the area, at 1.12 km space interval and a nominal flight altitude of 150 m approximately. The instrument used in the present aeromagnetic survey is the airborne fluxgate magnetometer type Gulf MK III, with a sensitivity of approximately one nT/mm. The diurnal variation and magnetic storms were recorded by means of the Gulf I ground magnetic storm monitor.

Geological Outlines

The area is a part of the African shield essentially of Precambrian age and is greatly covered by the igneous-metamorphic basement complex. It is an area of complicated geology due to its long history. The geology of the area as given here is based primarily on the geological map (Fig. 2) compiled from various sources mainly, the photogeological map prepared by Hunting (1967), the geological maps prepared by Soliman *et al.* (1978), Mansour (1972) and Qusa *et al.* (1978). The rocks in the study area are classified according to El Shazly (1964 and 1977).

First Basement Sediments or Geosynclinal Sediments

They are represented by regionally-metamorphosed impure limestones and dolomites with minor impure sandstones. The metamorphosed sediments are intercalated with metamorphosed volcanics and separated as well from the overlying volcanics by angular unconformity (Mansour 1972).

First Basement Volcanics or main Geosynclinal Volcanics

They are developed during the early stage of folding. They are represented in the study area by Sheikh Shadli metavolcanics with regionally-metamorphosed rhyolites, andesites, basalts and pyroclastic rocks. They are represented also by basic-ultrabasic association, which are relatively younger than Shadli metavolcanics and occur as dykes, sheets, stock intruding and interbedded with metasediments and Sheikh Shadli metavolcanic flows (Mansour 1972).

Second Basement Plutonites or Synorogenic Plutonites

These plutonites are developed during the main orogeny and are represented by granodiorites and diorites. They are notably mobile with abundant xenoliths and wide gradational contact zones. They are more basic and rich in plagioclase feldspars. These rocks have been considered by El Shazly (1966) as syntectonic or late tectonic.

Second Basement Volcanics or Emerging Geosynclinal Volcanics

The previous intrusive activity of synorogenic plutonites was followed by an extrusive sequence. They are formed of unmetamorphosed andesites, porphyrites, ignimbrites and other intermediate-acidic pyroclastics. They are considered by El Shazly (1964) as emerging geosynclinal volcanics or second basement volcanics El Shazly (1977) and by Sabet (1961) as post tectonic volcanics. They are known as Dokhan volcanics.

Second Basement Sediments or Postgeosynclinal Sediments and Associated Volcanics

They occupy basins and down-thrown areas scattered in the basement, which are normally represented by clastic beds of conglomerate, and mudstones of arkosic nature. They are known as Hammamat sediments.

Third Basement Plutonites or Late Orogenic Plutonites

These plutonites are mainly represented by intrusive red and pink granites, which possess sharp contacts (Ghanem 1968). Akkad and El Ramly (1961) believe that the granite plutons are not all of the same age, but they are of different members, intruded over a lapse of time. The plutonites are followed by the formation of pegmatites, aplites, felsites and quartz veins (El Shazly 1964 and 1977).

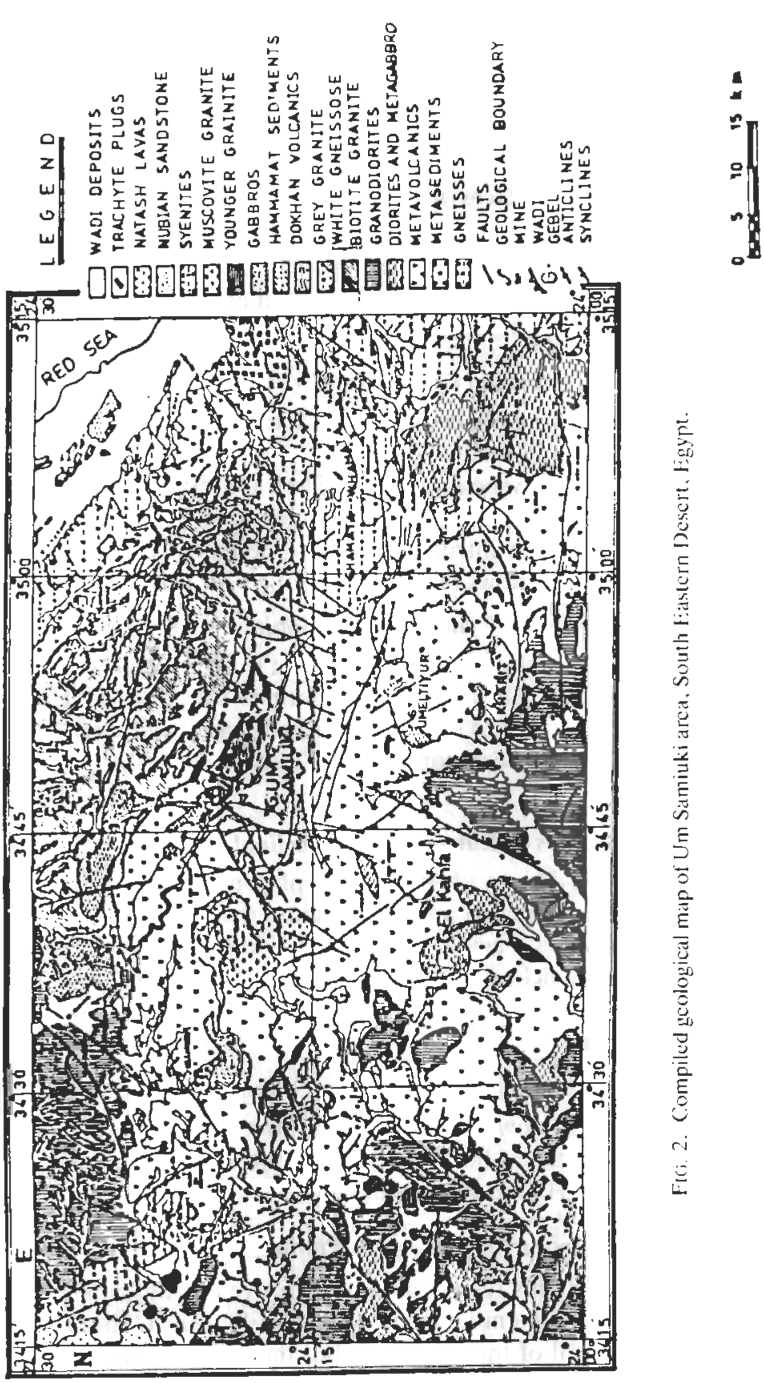

FIG. 2. Compiled geological map of Um Samiuki area, South Eastern Desert, Egypt.

Paleozoic Volcanicity or Postorogenic Volcanics

They are widely distributed in the basement cutting the previously-mentioned formations, but not the exposed sedimentary cover. They are usually termed post-granitic dykes. The main dyke varieties of this group are: andesites, trachytes, bostonites, camptonites, lamprophyres, and basalts. The bostonites are normally altered by hydrothermal solution (El Shazly 1964 and 1977).

Cretaceous Sediments or Third Detrital Sediments

They represent a part of the Nubian sandstone belt of the Eastern Desert of Egypt which extends northerly to Galala plateau at its northern part. The Nubian sandstones cover a considerable part of the Egyptian Desert. Their origin is doubtful and the stratigraphic position may be Cretaceous. They show a wide range of the sandstone type having various intercalations (Farag 1958).

Mesozoic Volcanicity or Alkaline Volcanics with Subordinate Plutonites

These are represented by several ring complexes as well as the alkalic volcanics of wadi Natash which are composed mainly of olivine basalts, mugearites, trachytes and phonolites.

Quaternary Sediments

They are represented by alluvial and proluvial loams, pebbles and sands of the Recent-upper Quaternary covering the wadies in the considered area.

Techniques of Analysis of Aeromagnetic Data

Reduction to the north magnetic pole (Baranov 1975)

Aeromagnetic data were corrected for the regional gradient of the Earth's magnetic field and reduced to the north magnetic pole (Fig. 3). The technique used in this transformation is that of Baranov (1975) and optimized by Fouad *et al.* (1981). It was found very useful in assessing the shapes and locations of the induced magnetized bodies, thus resulting in locating the peak of the anomalies more closely over the centres of the causative bodies.

Calculation of power spectrum for interface determination

The aeromagnetic data were interpreted by means of local power spectra suggested by Spector and Grant (1979), but avoiding the restrictions of the procedure as considered by (Cianciara and Marcak 1976). The power spectrum of an anomaly is calculated for the mean values of the Fourier transformation. By averaging over circles and anticipated spectrum value is determined. Using the assumed statistical properties of the parameter distributions Cianciara and Marcak (1976), determined geometrically the average depth of the distributions surface and the average thickness of the rectangular prisms of the model.

Two main average levels (interfaces) at depths 0.8 and 2.0 km below the measuring level were revealed through the application of power spectra (Fig. 4) on aeromagnetic map reduced to the north magnetic pole (Fig. 3).

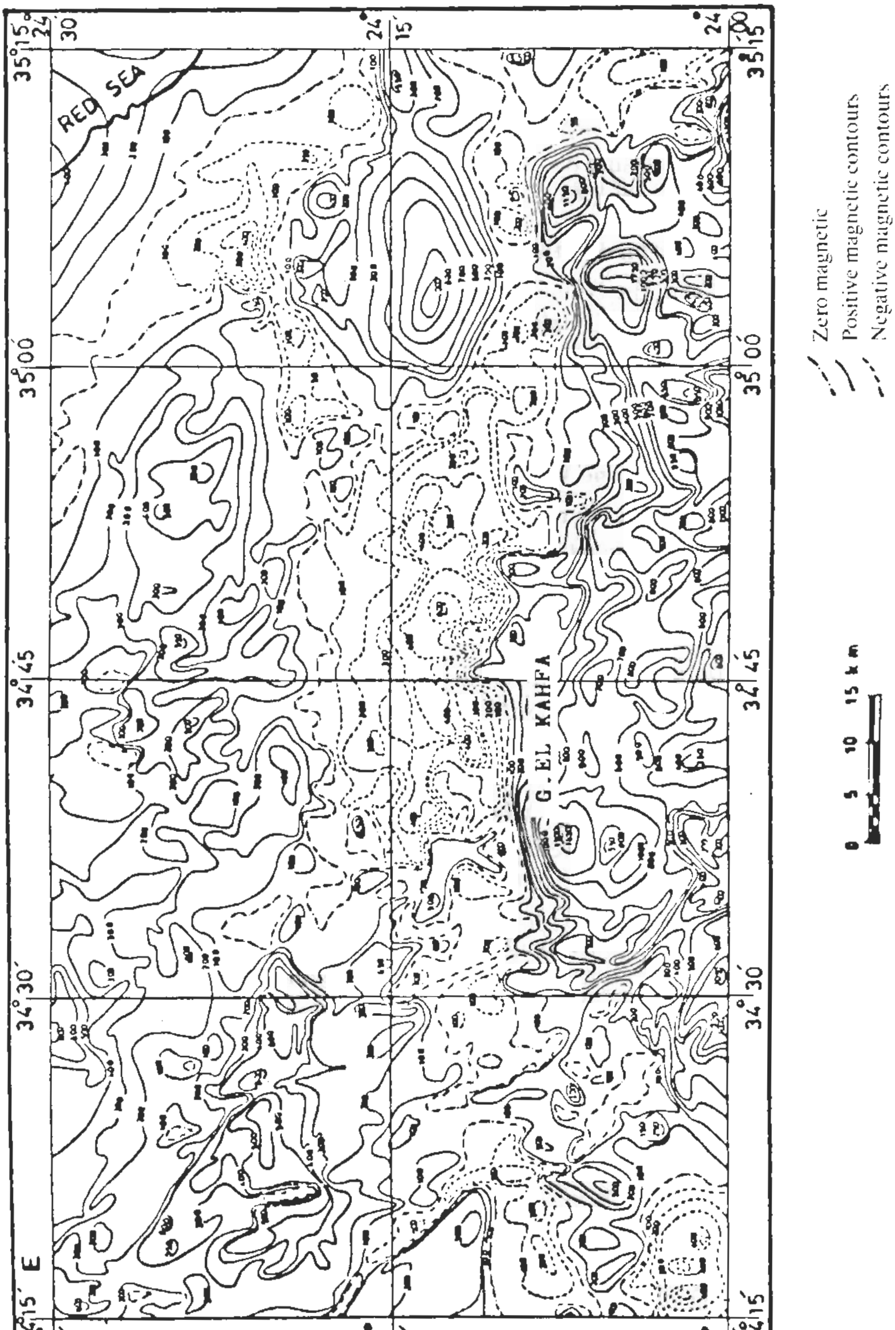

FIG. 3. Total aeromagnetic map reduced to the north magnetic pole of Um Samiuki area, South Eastern Desert, Egypt.

Filtering combined with the analytical downward continuation

Filtering of the RTP magnetic data was carried out using the analytical downward continuation (Cianciara and Marcak 1979).

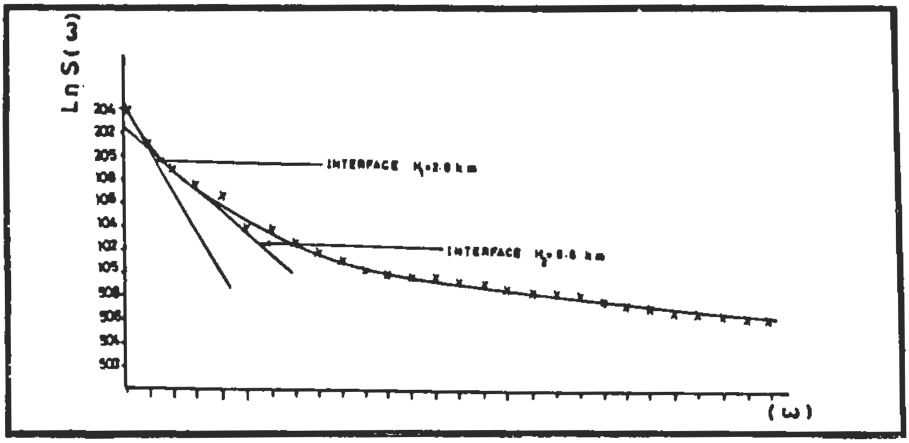

FIG. 4. Local power spectra for interface determination of Um Samiuki area, South Eastern Desert, Egypt.

Normalized total vector (gradient) of field intensity and phase angle

These two geophysical techniques were conducted on the RTP magnetic data based on the work of Harbough and Merriam 1968, as well as on the digital computer program worked out by Cianciara and Marcak 1979.

Statistical analysis of various trends

The overlap technique (Haugh, Brisbin and Turek 1967 and Johnson and Leone 1964) was carried out on all of the maps constructed and used in the present work (Figures 5, 6, 7, 8, 9, 10, 12 and 14), to define the regional structural framework of the area under study. This technique was based on the chi-squared test for data distributions. In this respect, a comparison of the observed data with an isotropic model was conducted, into which equal frequencies were expected in each of an arbitrary number of equal azimuth sub-divisions. If the hypothesis of random ordering is rejected, on a probability basis; a trend is then identified and its significance is tested at the 99% confidence level. The method applies the principle that a chi-squared distribution with a large number of degrees of freedom may be used in place of normal distribution, especially if an essentially-positive variable is to be represented. In this techniques, trends represented by peaks lying above the significance line are considered statistically significant at the 99% level of confidence, reflecting major or regional trends.

Trends that have been subjected to the statistical techniques of analysis are the structural lines as interpreted from the two total phase maps, as well as the magnetic gradients and the axes of magnetic anomalies as traced from the remaining (resulting) six magnetic maps. The length of each trend was measured to the nearest 0.1 km,

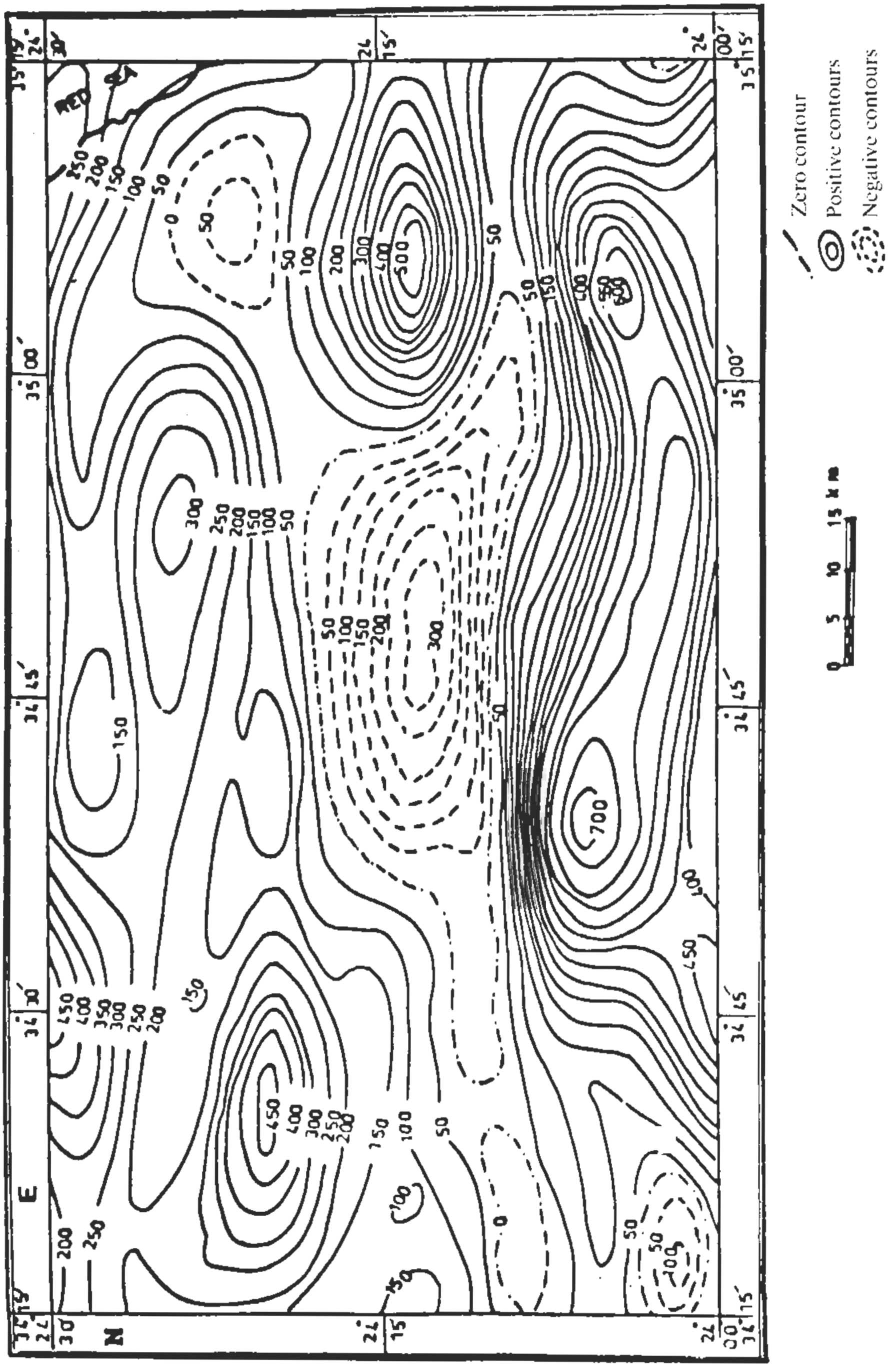

FIG. 5. Regional magnetic-component map reduced to the north magnetic pole at interface 0.8 km. of Um Samiuki area, South Eastern Desert, Egypt.

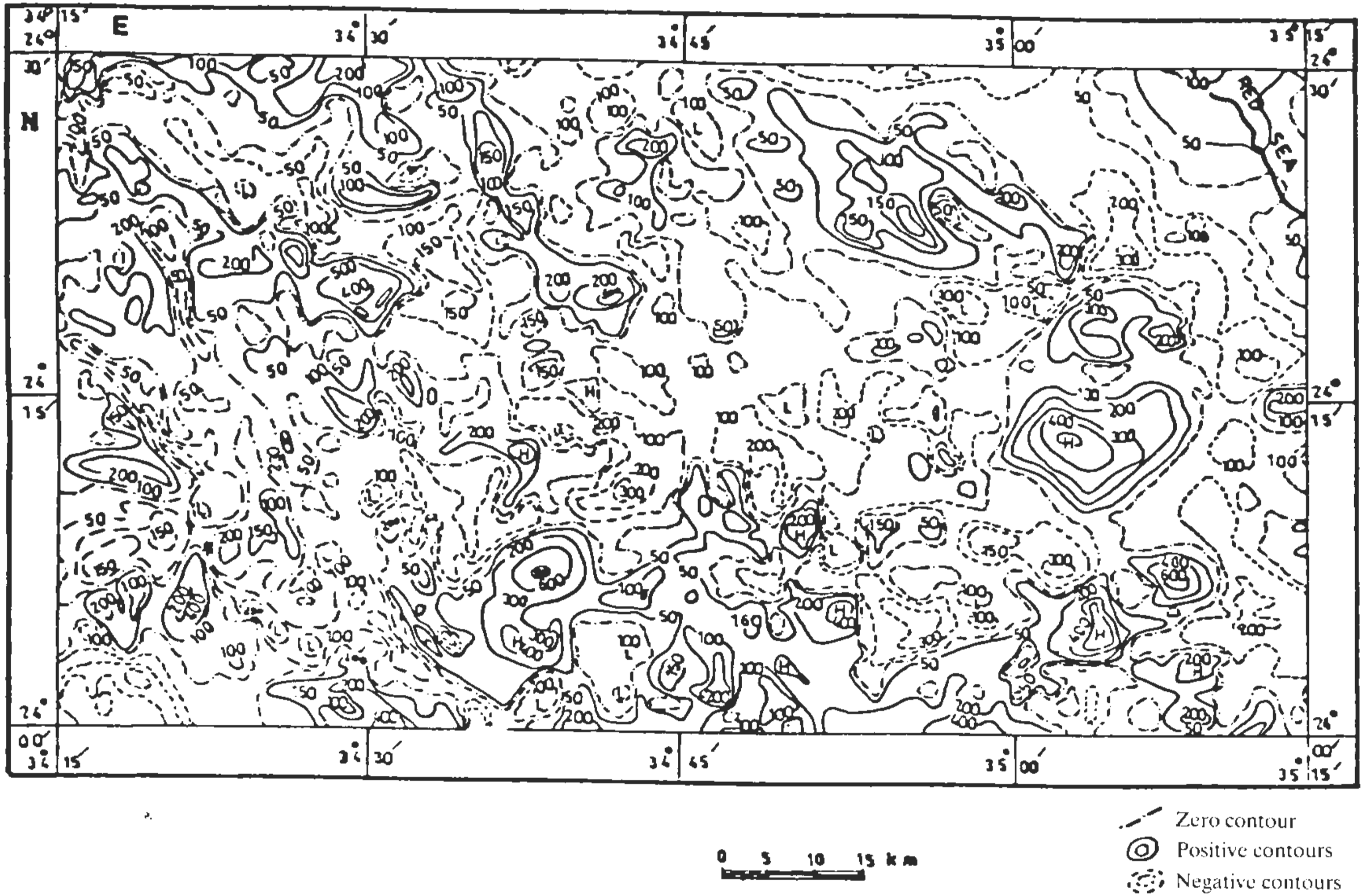

FIG. 6. Residual magnetic-component map reduced to the north magnetic pole at interface 0.8 km. of Um Samiuki area, South Eastern Desert, Egypt.

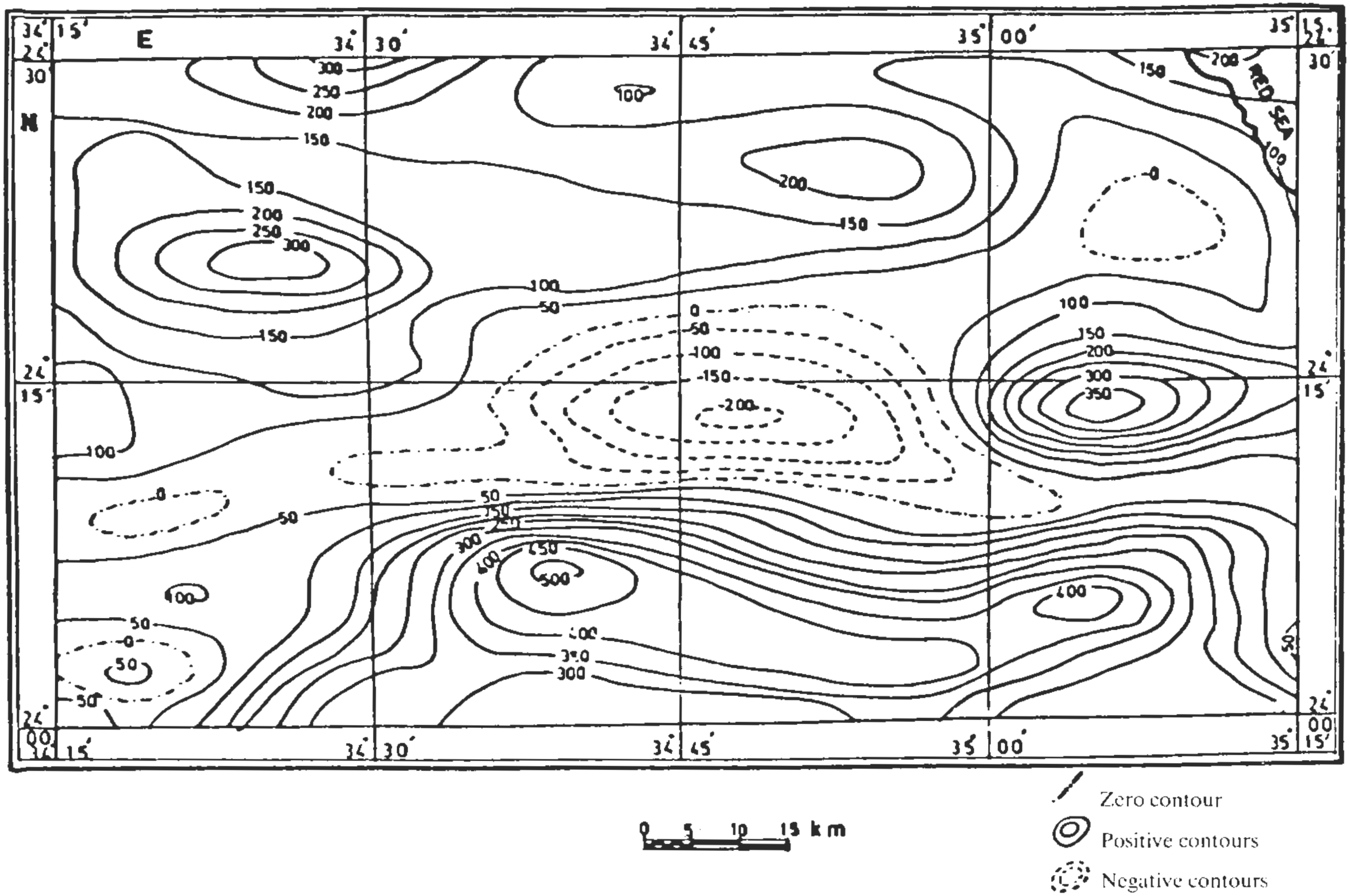

FIG. 7. Regional magnetic-component map reduced to the north magnetic pole at interface 2.0 km, of Um Samiuki area, South Eastern Desert, Egypt.

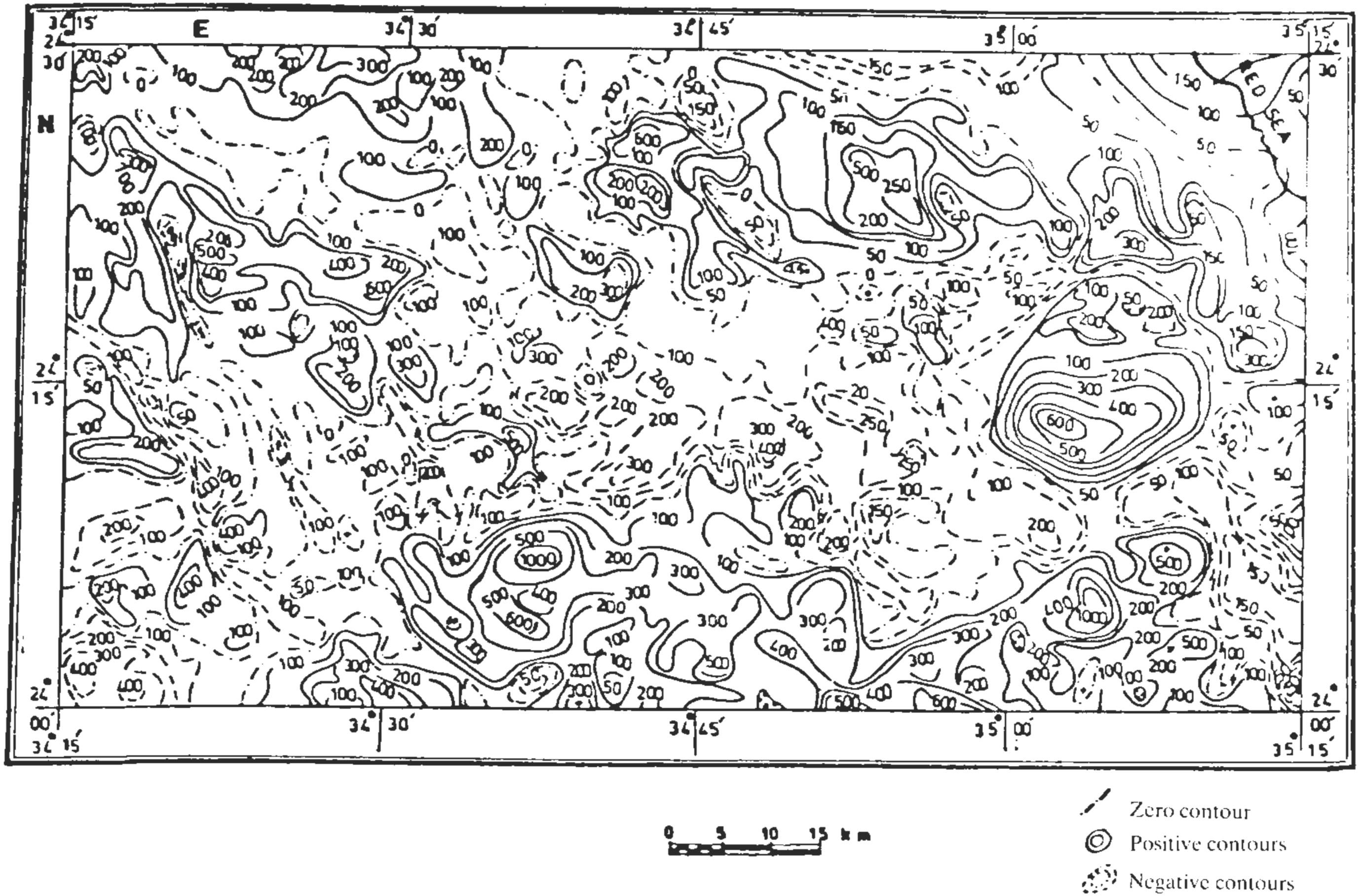

FIG. 8. Residual magnetic-component map reduced to the north magnetic pole at interface 2.0 km, of Um Samiuki area, South Eastern Desert, Egypt.

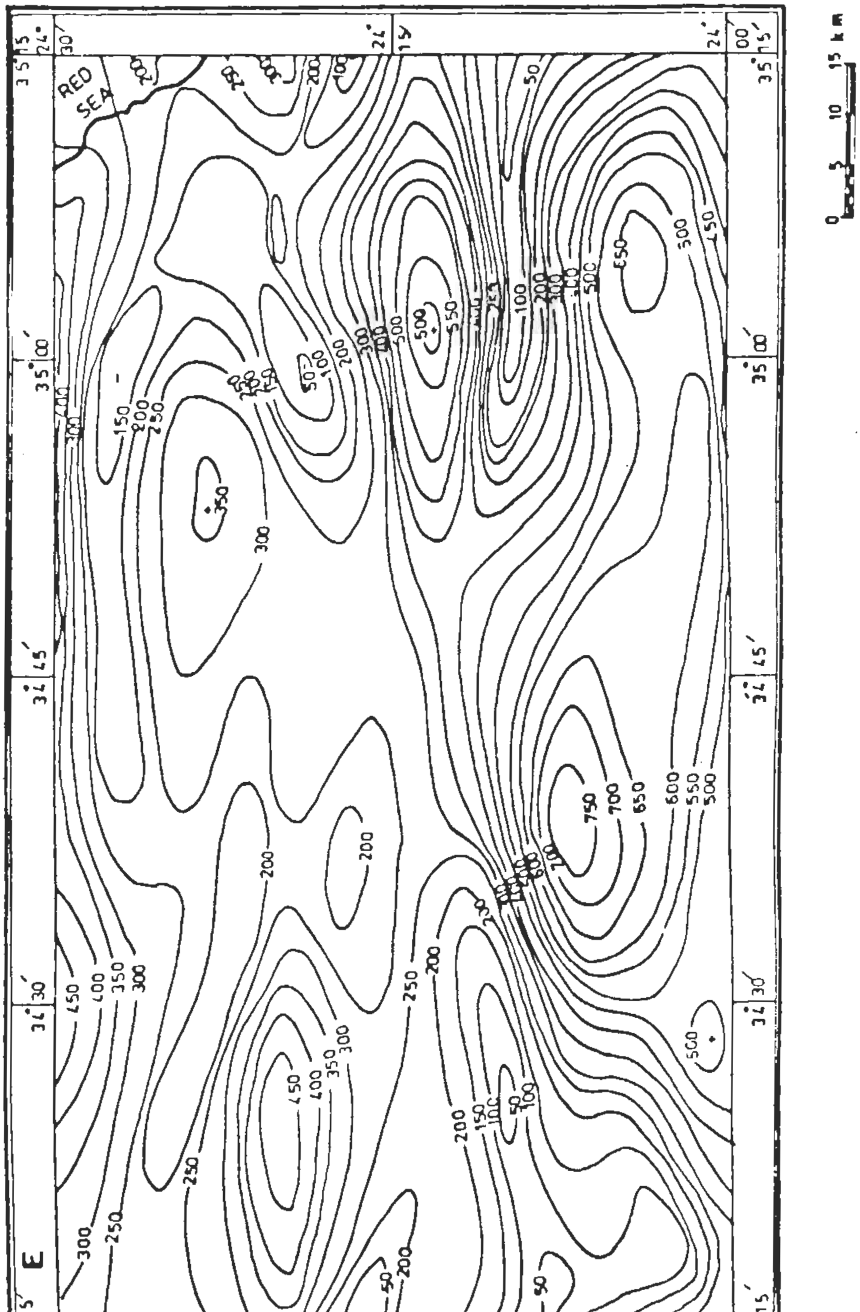

FIG. 9. Total gradient map at interface 0.8 km, of Um Samiuki area, South Eastern Desert, Egypt.

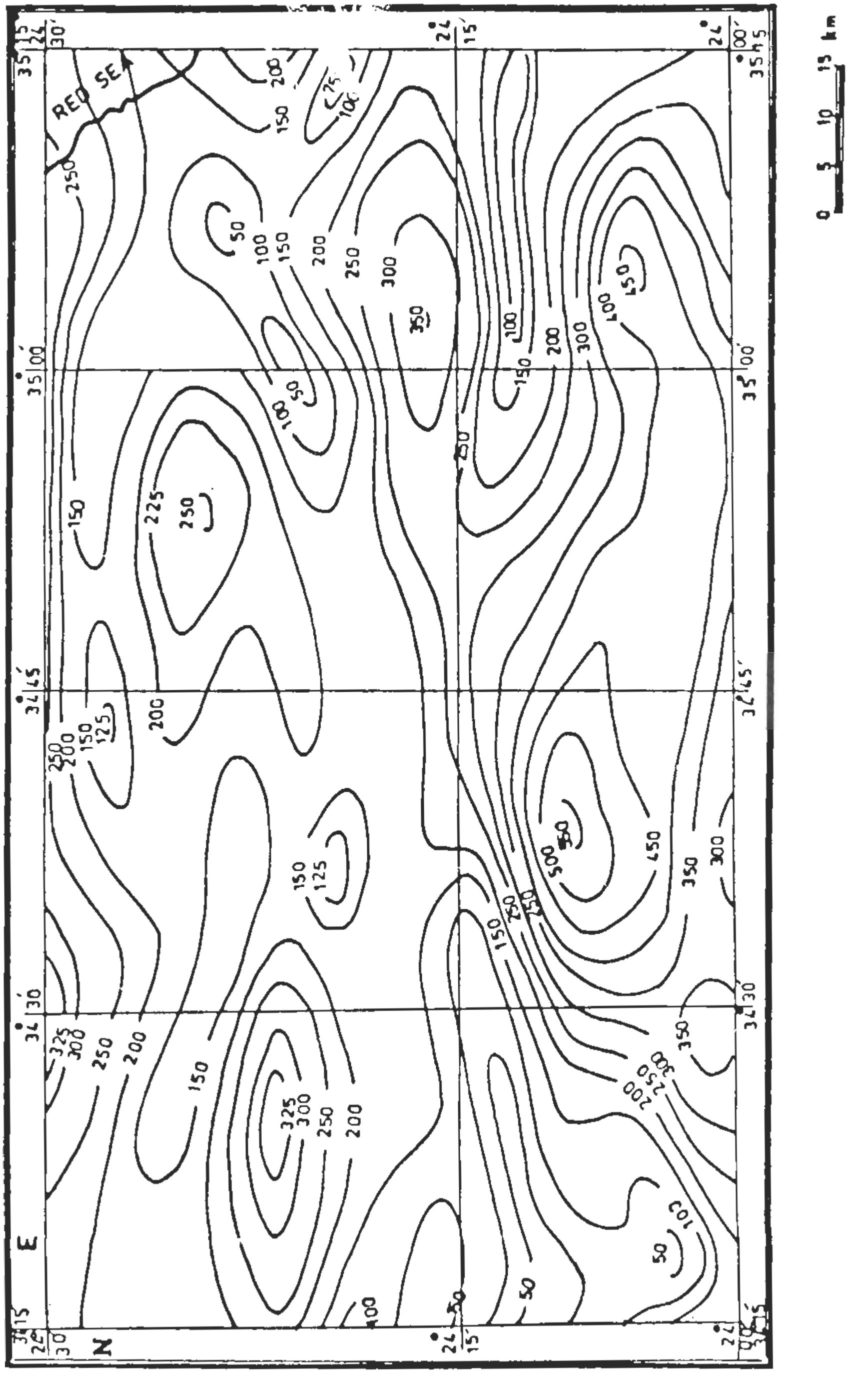

Fig. 10. Total gradient map at interface 2.0 km. of Um Samiuki area, South Eastern Desert, Egypt.

TABLE 1. The characteristic features of the various peaks of the magnetic-anomaly, magnetic gradient and structural trend patterns (Fig. 13 to 15).

Direction (in degrees)	Max. amplitude (in km. & in %)	Critical frequency (in km. & in %)	Half maximum width (in degrees)
I – Regional magnetic-component map,			
at interface 0.8 km. (Fig. 13a)		(12.0, 5.9)	
N 70° W	15.0 (very weak) 7.4		4° (very sharp)
N 85° W	116.0 (very strong) 56.9		5° (very sharp)
N 77° E	20.0 (weak) 9.8		4° (very sharp)
N 88° E	53.0 (strong) 25.9		5° (very sharp)
at interface 2.0 km. (Fig. 13c)		(9.5, 7.1)	
N 68° W	17.0 (weak) 12.7		4° (very sharp)
N 75° W	19.0 (moderate) 14.2		4° (very sharp)
N 85° W	74.0 (very strong) 55.2		7° (sharp)
N 85° E	24.0 (strong) 17.9		3° (very sharp)
II – Residual magnetic-component map,			
at interface 0.8 km. (Fig. 13b)		(23.0, 12.0)	
N 25° W	37.0 (strong) 19.3		9° (sharp)
N 40° W	57.5 (very strong) 30.0		7° (sharp)
N 50° W	71.5 (very strong) 37.2		6° (sharp)
N 60° W	26.0 (moderate) 13.5		3° (very sharp)
at interface 2.0 km. (Fig. 13d)		(15.5, 7.6)	
N 19° W	26.0 (weak) 12.8		6° (sharp)
N 26° W	22.5 (weak) 11.1		6° (sharp)
N 37° W	24.0 (weak) 11.8		4° (very sharp)
N 40° W	21.0 (weak) 10.3		4° (very sharp)
N 44° W	20.5 (weak) 10.1		4° (very sharp)
N 51° W	20.0 (weak) 9.9		3° (very sharp)
N 73° W	40.0 (strong) 19.7		4° (very sharp)
N 55° E	29.0 (moderate) 14.3		6° (sharp)
III – Total magnetic gradient map,			
at interface 0.8 km. (Fig. 14a)		(11.5, 3.9)	
N 90° W	120.0 (very strong) 40.8		6° (sharp)
N 66° E	15.0 (very weak) 5.1		4° (very sharp)
N 76° E	24.0 (weak) 8.2		4° (very sharp)
N 90° E	135.0 (very strong) 45.9		7° (sharp)
at interface 2.0 km. (Fig. 14b)		(13.5, 7.4)	
N 86° W	75.0 (very strong) 40.9		6° (sharp)
N 65° W	23.0 (weak) 12.6		3° (very sharp)
N 74° W	23.0 (weak) 12.6		3° (very sharp)
N 78° E	60.0 (very strong) 32.3		6° (sharp)
N 86° E	56.0 (very strong) 30.6		4° (very sharp)
IV – Basement tectonic map,			
Faults :			
at interface 0.8 km. (Fig. 14c)		(13.1, 10.4)	
N 40° W	21.5 (moderate) 16.1		6° (sharp)
N 47° W	15.5 (weak) 12.3		2° (very sharp)

TABLE 1. (continued.)

Direction (in degrees)	Max. amplitude (in km. & in %)	Critical frequency (in km. & in %)	Half maximum width (in degrees)
N 55° W	29.0 (strong) 22.9		6° (sharp)
N 68° W	23.0 (strong) 18.2		13° (broad)
N 52° E	18.5 (moderate) 14.6		13° (broad)
N 67° E	19.0 (strong) 15.0		4° (very sharp)
at interface 2.0 km. (Fig. 14d)		(12.9, 10.9)	
N 40° W	18.0 (moderate) 15.2		7° (sharp)
N 50° W	16.0 (weak) 13.5		9° (sharp)
N 63° W	31.0 (strong) 26.2		6° (sharp)
N 71° W	33.5 (very strong) 28.3		4° (very sharp)
N 67° E	20.0 (moderate) 16.9		13° (broad)
Folds :			
at interface 0.8 km. (Fig. 15a)		(22.5, 4.6)	
N 66° W	30.0 (very weak) 6.1		6° (sharp)
N 69° W	41.0 (weak) 8.4		3° (very sharp)
N 75° W	89.0 (strong) 18.3		4° (very sharp)
N 64° W	31.0 (very weak) 6.4		5° (very sharp)
N 73° E	67.0 (moderate) 15.1		3° (very sharp)
N 77° E	63.0 (moderate) 13.0		8° (sharp)
N 85° E	51.0 (weak) 10.5		5° (very sharp)
N 90° E	112.0 (strong) 23.1		6° (sharp)
at interface 2.0 km. (Fig. 15b)		(23.0, 6.2)	
N 65° W	39.0 (weak) 10.5		6° (sharp)
N 73° W	29.0 (very weak) 7.8		4° (very sharp)
N 64° E	28.0 (very weak) 7.5		6° (sharp)
N 72° E	58.0 (moderate) 15.6		7° (sharp)
N 74° E	76.0 (strong) 20.5		2° (very sharp)
N 80° E	75.0 (strong) 20.2		5° (very sharp)
N 90° E	65.0 (moderate) 17.5		6° (sharp)

and its direction was the angle measured clockwise from the geodetic north. Frequency trend distributions have been constructed with respect to their direction. Consequently, ten resultant frequency plots (Fig. 15 to 17) were prepared. The presence of various grouping of values "peaks", centered around definite directions on these curves make them more understandable. Correspondence and correlation were undertaken between the peaks of various plots.

Table 1 was prepared to classify and describe the characteristic features of peaks recorded over the ten plots, including direction from the north (eastwards and westwards), maximum amplitude (very weak, weak, moderate, strong, and very strong), half maximum width (very sharp, sharp and broad), and critical frequency (significance line) of every plot. In the present study, the peaks having less than 6° half-maximum width were considered very sharp, while those possessing 6° and more were treated as sharp and those possessing more than 10° were treated as broad ones. The maximum amplitude (intensity) of the peaks, on the other hand, were described as very weak, weak, moderate, strong and very strong, when they fluctuate from 3.0 to 7.5%, 8.0 to 12.5%, 13.5 to 17.5%, 18 to 26.5%, and 27.0 to 57.0% respectively.

Table 2 summerizes the magnetic-tectonic trends and their representative peaks on the ten frequency plots correlated with the general terminology adopted by various authors in NE Africa and Arabia (Schandelmeie *et al.* 1987, Abdel Gawad 1969, El Gaby 1983, El Shazly 1966, Halsey 1975, Krs *et al.* 1973, Meshref and El Sheikh 1973, Riad 1977 and Youssef 1968). The Gulf of Suez trend was proposed to include the north-northwest (N11.25°-33.75°W) and northwest (N33.75°-56.25°W) trends, suggested on geometrical basis (Fig. 18). Similarly, the remaining trends: the west northwest of Najd (N56.25°-78.75°W), the Tethyan (N78.75°W-N78.75°E), the trans African (N33.75°-56.25°E) and the Syrian arc or Qattara (N56.25°-78.75°E) were also treated in the same manner.

Qualitative Interpretation

Magnetic anomalies can be produced by a number of causative features such as lithology changes, variations in the thickness of magnetic units, faulting, folding and topographic relief. A significant amount of information can, at times, be obtained from a qualitative review of total magnetic-intensity and reduced-to-the pole maps. Magnetic anomaly frequency can be related to the distance between anomalous sources and the magnetic sensor. Given the same rock type, shallow sources produce higher frequency anomalies, while deep sources yield broader ones. At the same time, sufficiently large rock units can be recognized by characteristic anomaly patterns and anomaly amplitudes. The discrimination between various rock units can be based on different anomaly amplitude, frequency, orientation and general intensity levels (Aero-Service report 1984b).

Aeromagnetic surveys show various geological structures such as: folds, faults and deep-seated tectonic structures, as well as, zones and blocks in the earth's crust. They could also delineate the ring structures and complexes as well as the basic and ultrabasic rock bodies. Other structures produce characteristic anomalies which have various expressions on the magnetic maps.

To reduce the influence of the inclination of the earth's magnetic field on the shapes, sizes and locations of the anomalies, reduction to the north magnetic pole of the aeromagnetic data has been carried out (Fig. 3). This reduction helped to assess more accurately the magnetized sources, and to identify the significant magnetic zones of anomalies of unusual amplitude and gradient. This reduction has served; to position the peaks of the anomalies more nearly over the centres of causative bodies and to identify bodies which are characterized by significant remanent magnetization.

The correlation between the magnetic features and compiled geological map was found to be generally very poor. In some instances, a well-defined magnetic gradient (contact or fault) would transgress several geologically-mapped contacts on the geologic map. One of the explanations for this discrepency, would be that the magnetic effect of the local or near-surface geological features and the deep geological

TABLE 2. The magnetic-tectonic trends and their representative peaks on the ten frequency plots prepared from the eight magnetic and tectonic basement maps, Gabal Um Samiuki area, South Eastern Desert, Egypt.

Trends \ Maps & Plots		Regional-component (Figures 5 & 7)		Residual-component (Figures 6 & 8)		Total gradient Figures 9 & 10)		Basement tectonics (Figures 18 & 19)			
		Interface (in km)									
								Faults		Folds	
Adopted terminology	General direction	0.8 (Fig. 13 a)	2.0 (Fig. 13 c)	0.8 (Fig. 13 b)	2.0 (Fig. 13 d)	0.8 (Fig. 14 a)	2.0 (Fig. 14 b)	0.8 (Fig. 14c)	2.0 (Fig. 14d)	0.8 (Fig. 15a)	2.0 (Fig. 15b)
Meridional	N-S (N11.25°W-N11.25°E)	M	i	n	o	r	T	r	e	n	d
Gulf of Suez-Red Sea	NNW-SSE (N11.25°-33.75°W)	– –	– –	N25°W –	N19°W N26°W	– –	– –	– –	– –	– –	– –
	NW-SE (N33.75°-56.25°W)	– – – –	– – – –	– N40°W N50°W –	N37°W N40°W N44°W N51°W	– – – –	– – – –	N40°W N47°W N55°W –	N40°W N50°W – –	– – – –	– – – –
Najd	WNW–ESE (N56.25°-78.75°W)	N70°W – –	N68°W N75°W –	– – –	N73°W – –	– – –	N65°W N74°W –	– N74°W –	N63°W N71°W –	N66°W N69°W N75°W	N65°W N73°W –
Tethyan	E-W (N78.75°W-N78.75°E)	N85°W N88°E	N85°W N85°E	– –	– –	N90°W N90°E	N86°W N87°E	– –	– –	N85°E N90°E	N80°E N90°E
Syrian or Qattara	ENE-WSW (N56.25°-78.75°E)	N77°E – –	– – –	– N60°E –	– – –	N66°E N76°E –	N78°E – –	N67°E – –	N67°E – –	N64°E N73°E N77°E	N64°E N72°E –
Trans-African	NE-SW (N33.75°-56.25°E)	– –	– –	– –	N55°E –	– –	– –	N52°E –	– –	– –	– –
Aqaba	NNE-SSW (N11.25°-33.75°E)	M	i	n	o	r	T	r	e	n	d

structures is different. It was found that strong magnetic anomalies of near-surface origin obscure the relatively weaker effects associated with deeper structures.

The RTP map (Fig. 3) of the area under investigation is characterized in its western portion by a series of linear aeromagnetic anomalies. They have pronounced amplitude, azimuthal orientation varying between N30°W and N35°W, running almost parallel to the Red Sea for more than 50 kms, and continuing beyond its limits. These linear anomalies were verified by ground geophysical methods (Krs and Other 1973), and were found to be caused by dykes containing a high proportion of ferromagnetic components.

Another feature observed on the RTP map (Fig. 3) is the presence of a strong and approximately circular magnetic anomaly at the south-west central portion of the study area. It is associated with Gabal El Kahfa ring complex and reaches in amplitude 1650 nT. In addition, the RTP map (Fig. 3) shows some aeromagnetic anomalies of large areal extent lying in the northeastern portion of the area under study. These anomalies related to a small portion of the Red Sea are of relatively large size and are characterized by weak amplitudes ranging between 150 and 400 nT. Meanwhile, the other magnetic anomalies met with over the land to the west of the Red Sea Coast, show relatively higher magnetic amplitudes.

The RTP map (Fig. 3) shows a very large E-W trending zone of magnetic lows lying at the central portion of the area, and is associated with metavolcanics. This low zone is bounded from the south and north by two major belts of magnetic highs.

The RTP map (Fig. 3) was separated using the analytical downward continuation (Cianciara and Marcak 1979) to present individually: (a) the magnetic effects of the magnetized materials near ground level (near-surface); and (b) the magnetic effects of deeply-buried magnetized materials (deep-seated). The resulting two magnetic-component maps were interpreted in terms of the lithology and structure. Deep major structures could be resolved and interpreted through the regional magnetic-component map. Two main average levels (interfaces) at depths 0.8 and 2.0 km below the measuring level were revealed through the application of power spectra (Fig. 4) on aeromagnetic map reduced to the north magnetic pole (Fig. 3). The result of analytical downward continuation is the filtering of the magnetic effects of the near-surface bodies from that of the deep-seated ones. Four maps were drawn (Figures 5, 6, 7 and 8) two at each level (interface): one for the regional- and the other for the residual-magnetic component.

The residual or near-surface magnetic-component maps (Figs. 6 and 8) at the two specified (interfaces) show a great similarity to the RTP map (Fig. 3). This observation may suggest that most of the basement rocks in the study area, responsible for the magnetization, are either outcropping or buried at a shallow depth. The residual maps in their western portion clearly show the characteristic linear magnetic anomalies, normally and reversely magnetized, associated with the deep-seated diabase dyke (Lockwood 1968), that trends in a northwestern direction. Moreover, the two residual maps show linear magnetic anomalies in their eastern portion similar to those found in their western portion, both in character and trend. The appearence of these linear anomalies on these maps in the east and their absence on the original (RTP) ones refer to their location at depth. This leads to the conclusion that the eastern part of the area is deeper than its western one.

In the southeastern corner of the area under study, a characteristic magnetic feature included within the southern zone of magnetic highs-very much similar to that recorded over G. El Kahfa ring complex- is revealed from the filtered maps. This feature does not correlate well with the geology in this part. Consequently, could be found at depth at the intersection of the NW and NE magnetic trends.

The regional magnetic-component maps (Figs. 5 and 7) at the assigned interface (levels) are the result of the removal of the anomalies corresponding with the intrusives from the recorded aeromagnetic anomalies. These two maps show the east-west trending axes of the positive and negative counterparts of the anomalous zones. The sharp, linear and conspicous, northwest-southeast trending (diabasic) anomalies are not represented completely (either westwards or eastwards) on the two regional maps. They show a low zone (ranging in amplitude from zero to –300 nT) located in the center of the study area and associated with Shadli metavolcanics. This low zone is surrounded from all sides by huge belts of magnetic highs, except the western side.

Figures 9 and 10 represent the distribution of the isolines of the total vector magnitude $G_i^p(z)$ in the study area at the two interfaces. The total gradient maps show closed isolines (anomalies) and disturbances of the isolines are related to the real sources at each level. Besides, it was possible from the total vector maps to delineate some structures as faulting (down-faulted and uplifted blocks) and folding (synclines and anticlines). The closures having highest values were interpreted as uplifted blocks (or anticlines) and the closures possessing lowest values were interpreted as subsided blocks (or synclines). The axes of these mapped blocks (or folds) correlated well with the elongation of these closures.

Figures 11 and 13 show the variation in the computed phase angle at the two assigned levels (interfaces) in the area under study. It was possible to exactly locate the faults, fault zones as well as the extension of bodies having the same magnetic characteristics, through the use of the bends (or sharp dislocations and the closures in the contour lines respectively.

Quantitative Interpretation

Magnetic Trend Analysis

The study of the character of magnetic anomalies is considered a common quantitative approach to magnetic interpretation. The character of the magnetic anomalies is based on amplitude, wave length, grouping of anomalies and their trend pattern. It has been shown that the trend patterns can be used to define magnetic provinces (Affleck 1963 and Hall 1964).

Statistical analysis of the directions of the magnetic lineaments interpreted from the six magnetic and two basement tectonic maps were not found to be randomly distributed but show six well-defined trends (Figs. 15 and 16). The results of these

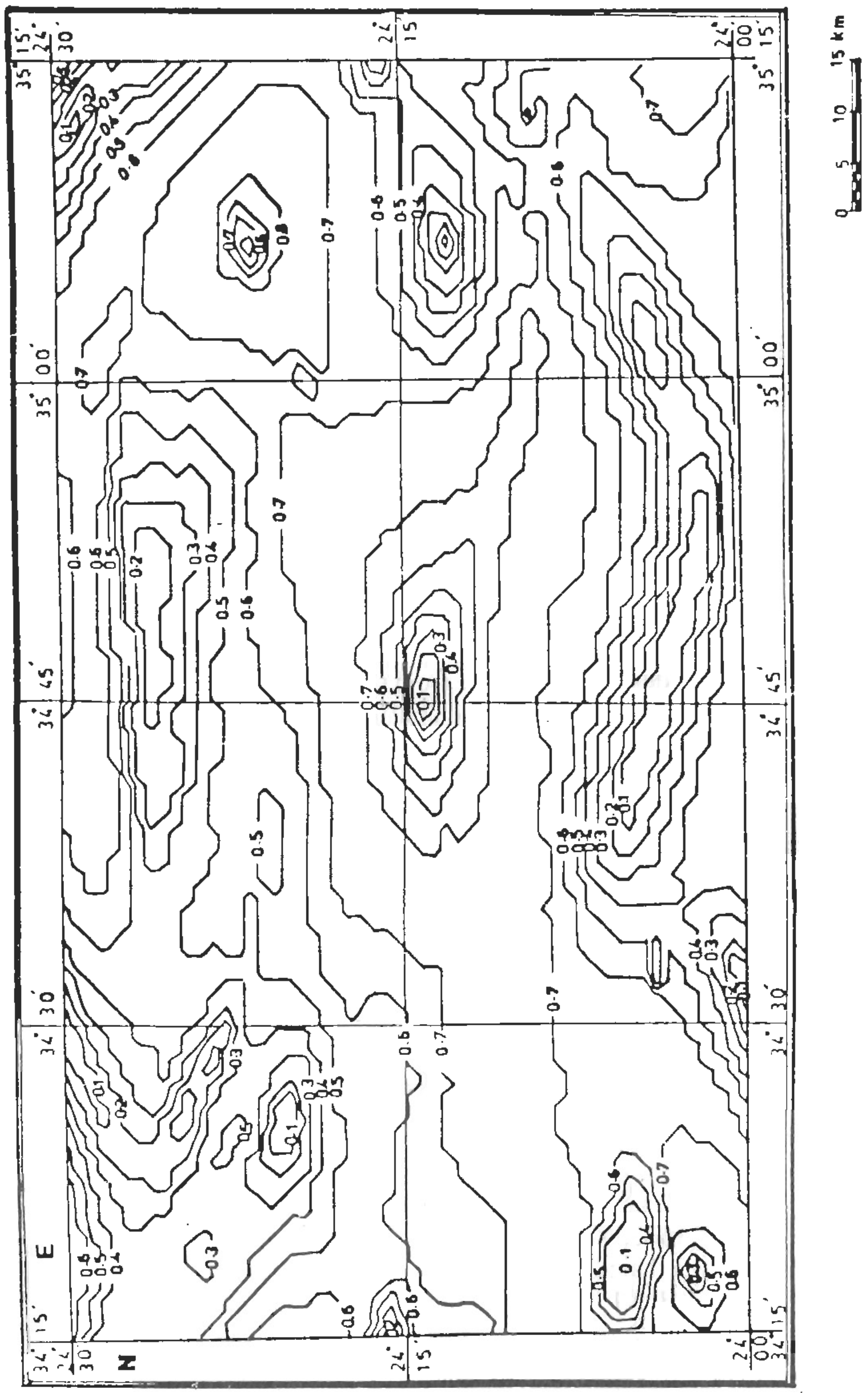

FIG. 11. Total phase angle map at interface 0.8 km. of Um Samiuki area, South Eastern Desert, Egypt.

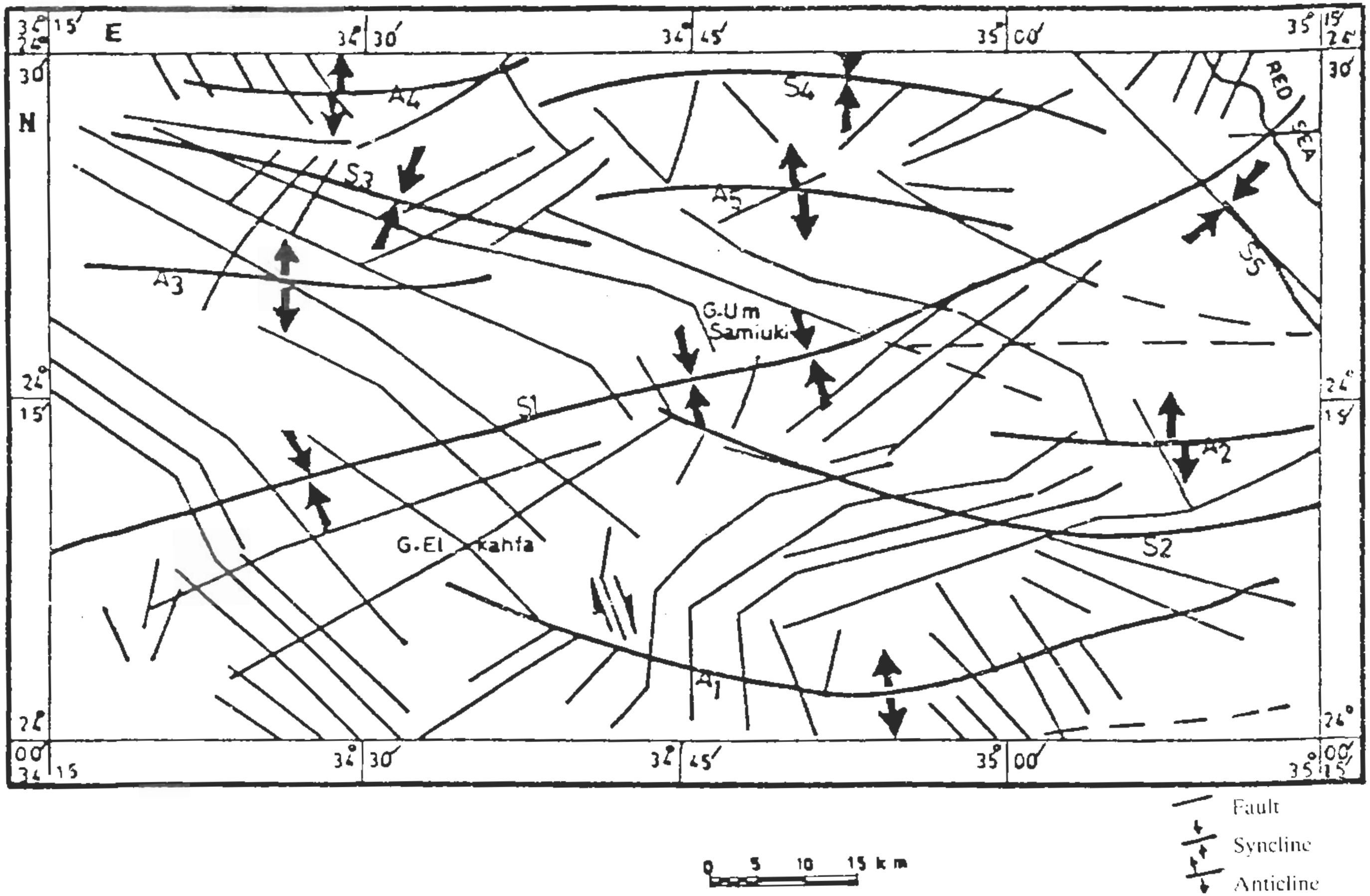

FIG. 12. Basement tectonic map as interpreted from total phase angle and total gradient maps at interface 0.8 km, Um Samiuki area, South Eastern Desert, Egypt.

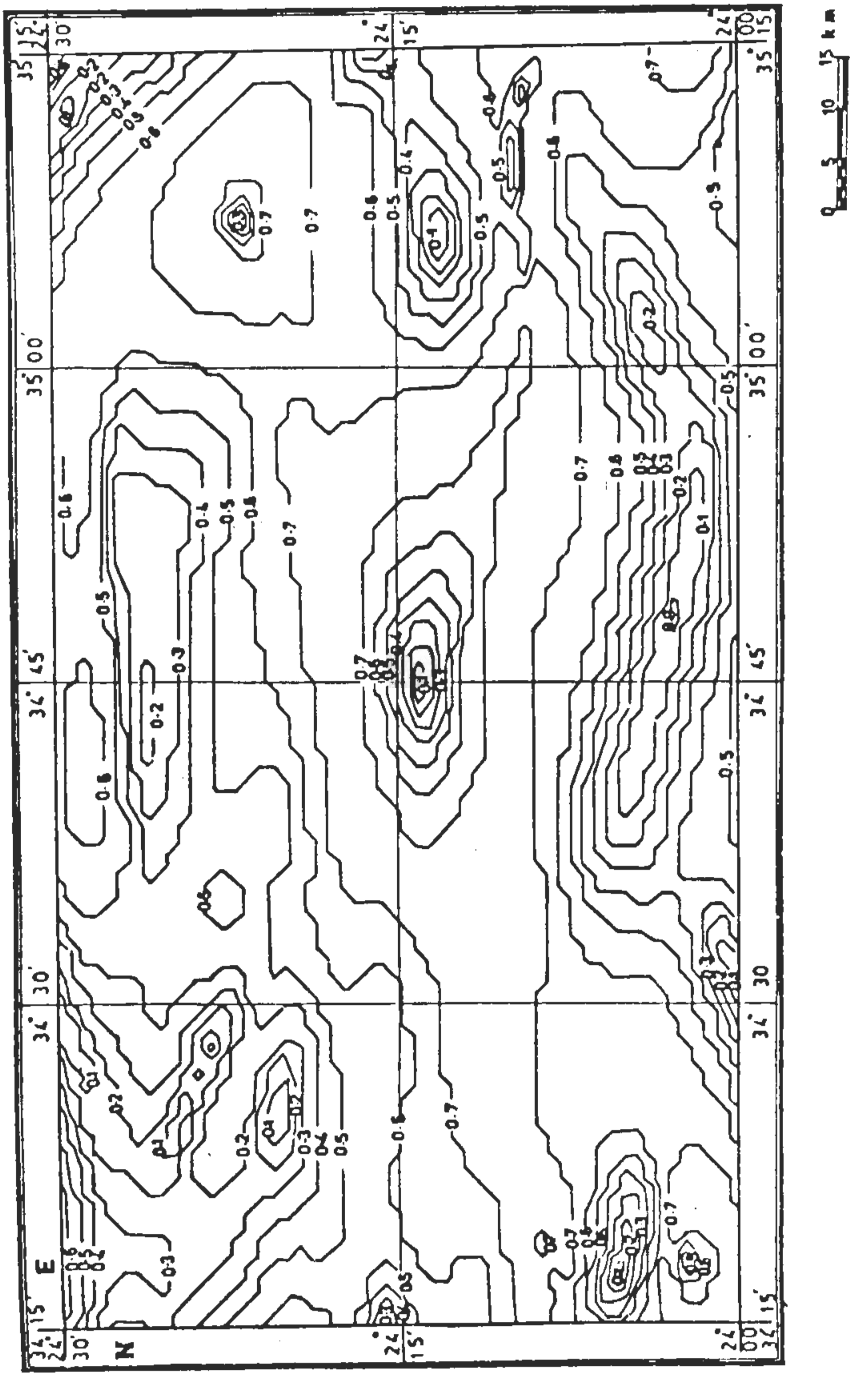

FIG. 13. Total phase angle map at interface 2.0 km, of Um Samiuki area, South Eastern Desert, Egypt.

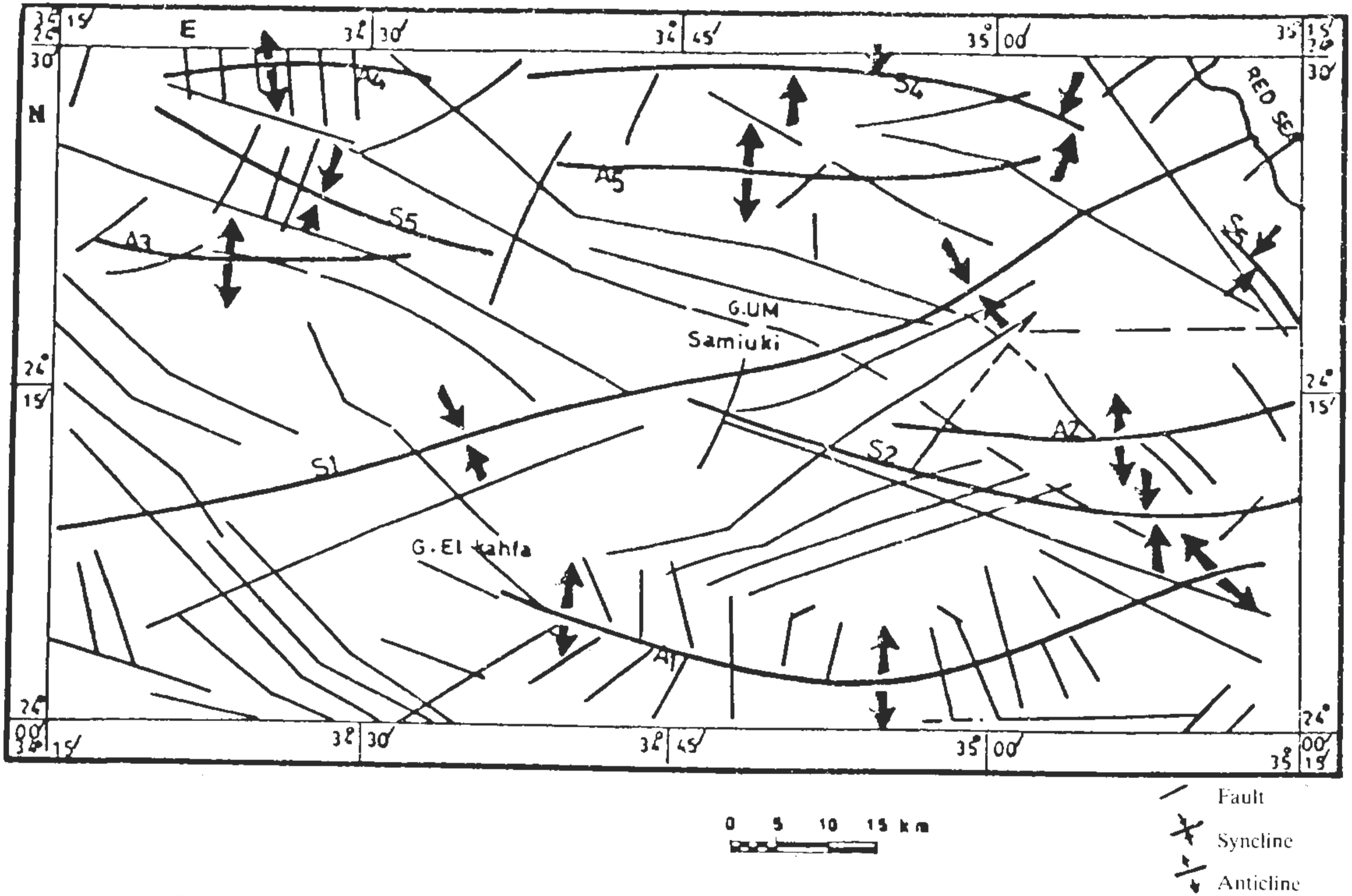

FIG. 14. Basement tectonic map as interpreted from total phase and total gradient maps at interface 2.0 km, Um Samiuki area, South Eastern Desert, Egypt.

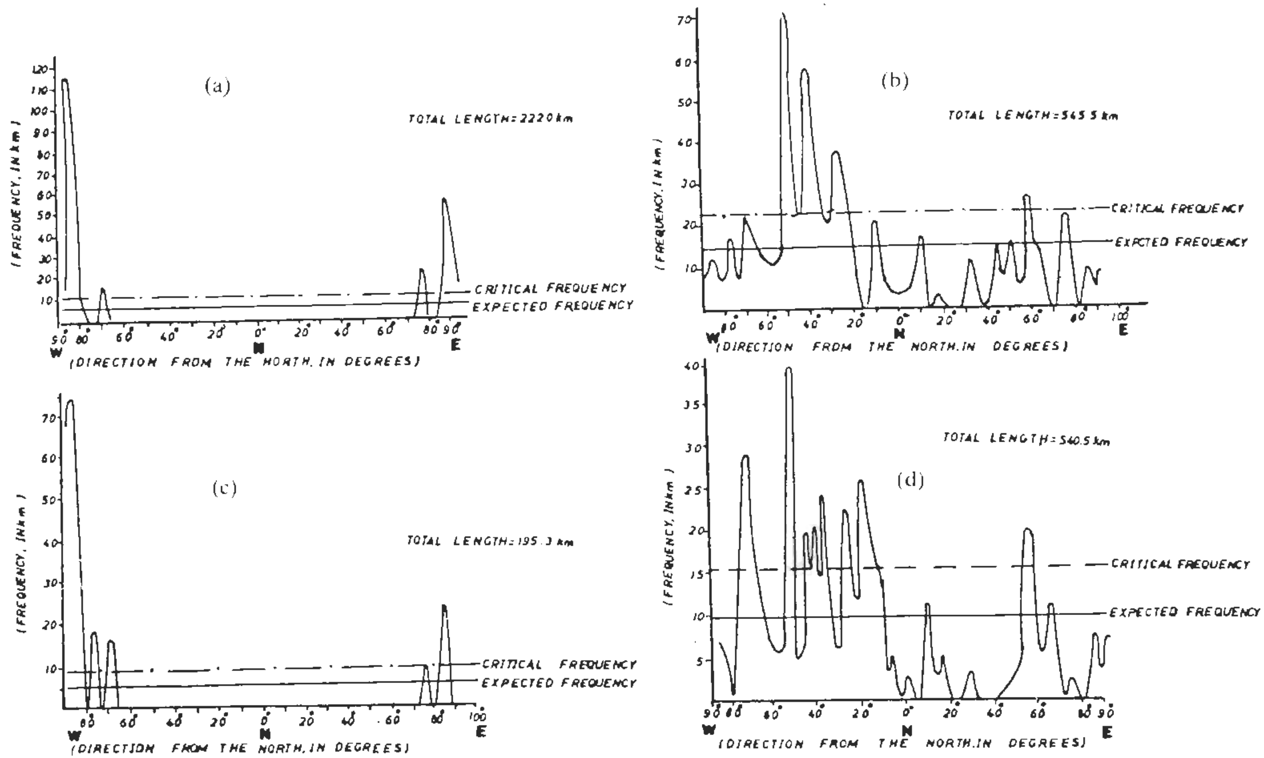

FIG. 15. Frequency distribution curves of the trends of magnetic lineaments, Um Samiuki area, South Eastern Desert, Egypt.

a – Regional magnetic component map at interface 0.8 km.
b – Residual magnetic component map at interface 0.8 km.
c – Regional magnetic component map at interface 2.0 km.
d – Residual magnetic component map at interface 2.0 km.

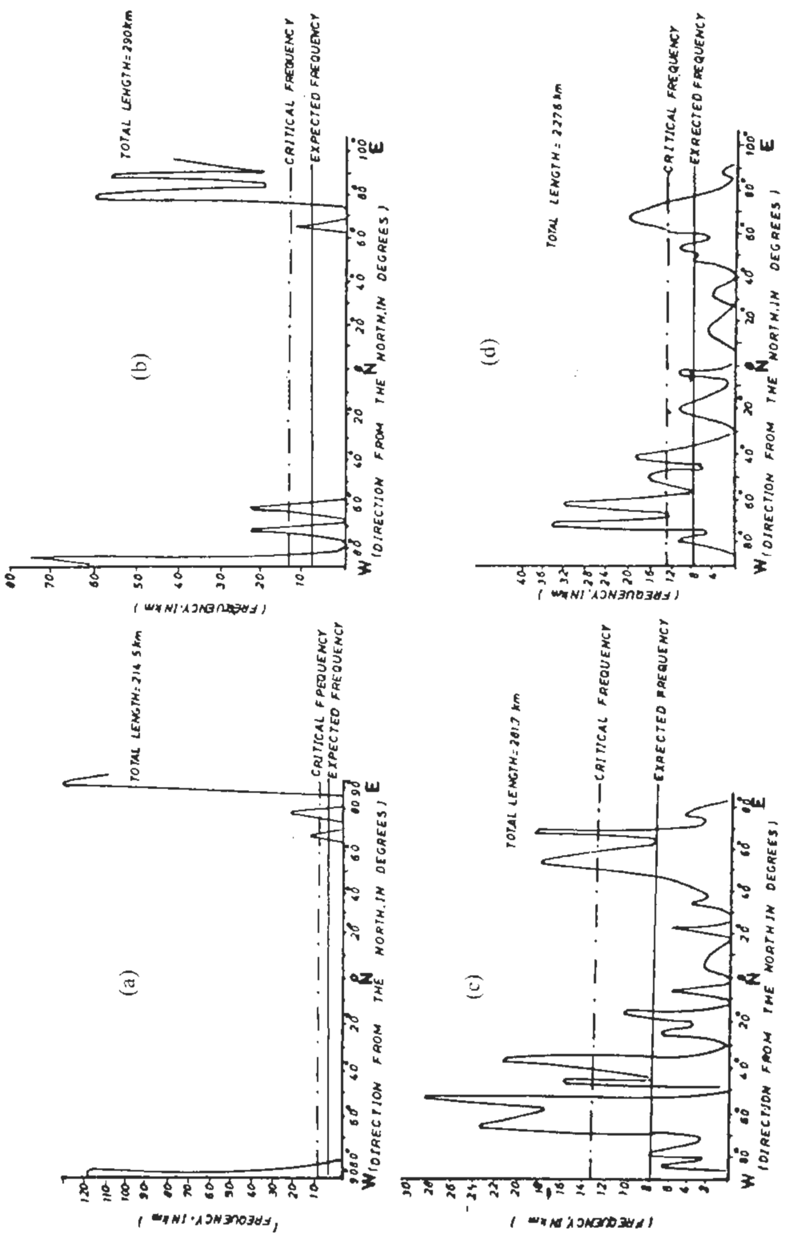

FIG. 16. Frequency distribution curves of the trends of magnetic lineaments, Um Samiuki area, South Eastern Desert, Egypt.
a – Total gradient map at interface 0.8 km.
b – Total gradient map at interface 2.0 km.
c – Phase angle map at interface 0.8 km.
d – Phase angle map at interface 2.0 km.

analyses were summarized in Table 2 which shows the major magnetic trends in the Gabal Um Samiuki area.

The discussion will be classified under five main categories according to azimuth, and follows this particular sequence: Gulf of Suez-Red Sea (NNW and NW) trend, Najd (WNW) trend, Tethyan (E-W) trend, Syrian arc or Qattara (ENE) trend and Trans African (NE) trend.

Gulf of Suez-Red Sea (NNW-SSE and NW-SE) trend

This category is the richest between the other categories concerning the number of recorded peaks; since it plays an important role in the structural framework of Egypt. It was observed that the NW-SE trend is well developed on the frequency plots interpreted from the residual-component and basement tectonic maps at the two interfaces and is lacking on the remaining plots (Fig. 5, 7, 9 and 10). The NNW-SSE trend was recorded only on the frequency plot of the residual-component maps (Fig. 6 and 8).

The characteristic features of the different peaks of this trend registered over the different frequency plots are shown in Table 1.

The Gulf of Suez-Red Sea trend may represent the more developed set, out of two sets of shear fractures produced by the hypothetical stress directed approximately N-S, that accompanied the formation of the rift system associated with the Red Sea (Ammar *et al.* 1983).

The northern part of Egypt is mainly covered by younger sediments. Where Paleozoic strata are exposed, the regional frame of structural development is too small to draw general conclusions, especially because young structural displacements (Gulf of Suez, Red Sea) are parallel to the structural relief of the Paleozoic system (Schandelmeier *et al.* 1987).

Ammar *et al.* 1983, stated that, from the mineralization emplacement point of view, the N35°W trend may be considered important for the Phanerozoic cover sediments, while the N45°W trend could be regarded of great value concerning the Precambrian Basement rocks.

The interpretation of the Bouguer anomaly map of the northern part of Egypt by Riad (1977), has shown the presence of almost parallel shears striking in a NW-SE direction which are probably related to the interaction of the European and African plates. The results of the quantitative analysis of the structural data in the Central Eastern Desert of Egypt (El Shazly *et al.* 1980) has defined a simple stress pattern oriented so as the maximum principal axis directed nearly NE-SW.

The NW-SE trend seems to be the most important among all other trends, and plays the most important role in the structural framework of mineralization emplacement in the Central Eastern Desert of Egypt (Ammar *et al.* 1983).

This trend is developed mainly on the residual magnetic-component (near-surface) maps and lacking on the regional magnetic-component (deep-seated) map.

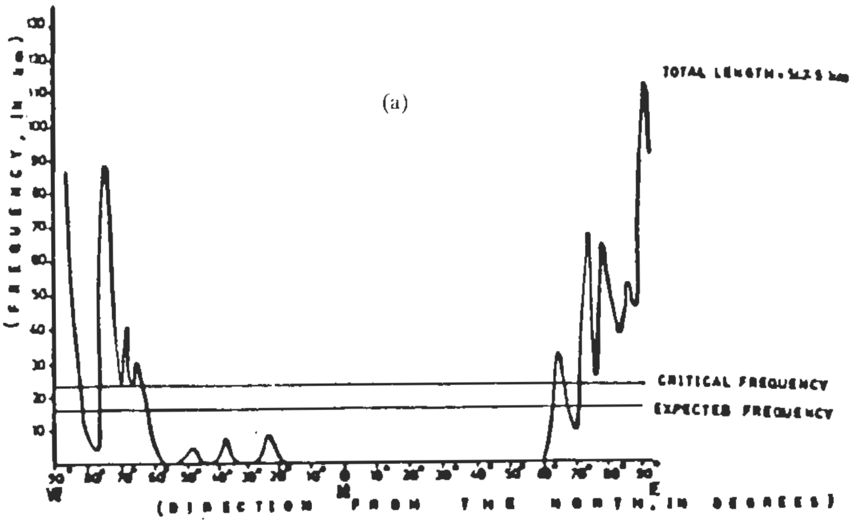

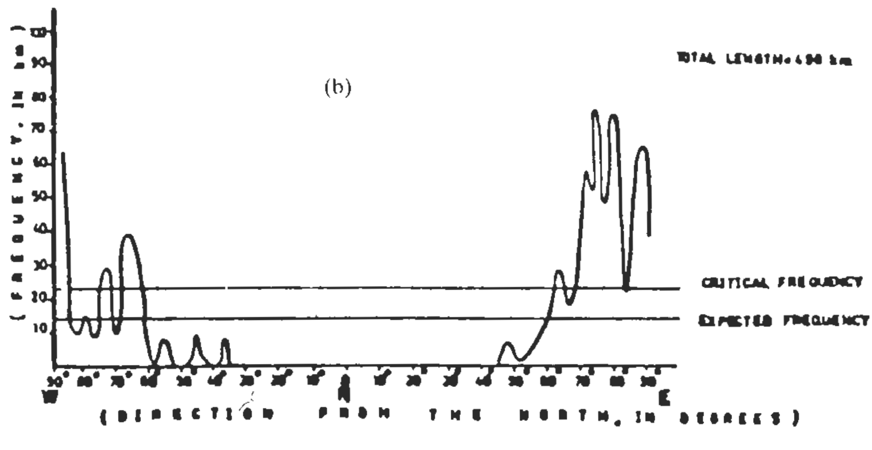

FIG. 17. Frequency distribution curves of the interpreted basement folds at interface 0.8 km (a) and 2.0 km (b), Um Samiuki area, South Eastern Desert, Egypt.

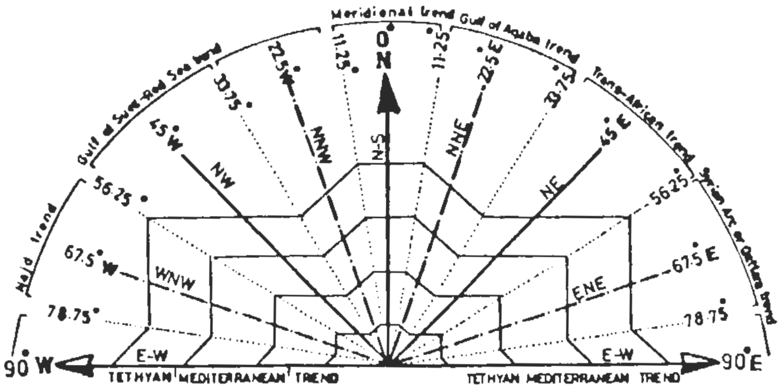

FIG. 18. Suggested general geometrical classification of the various directions in correlation with the terminology of main structural trends adopted by various authors in north-east Africa and Arabia.

This is in contrary to what was observed concerning the Tethyan (E-W) trend. This observation led to the conclusion that this trend is younger than the Mediterranean (E-W) one. The NNW-SSE trend is represented only on the frequency plots of the residual magnetic-component map and is not represented on any plot of the other maps. This means that this trend is of minor importance as far as the area is concerned.

Najd (WNW-ESE) trend

The characteristic features of the various peaks (representing the WNW-ESE trend) gathered from the various frequency plots are described separately in Table 1.

This direction is recognized as a possible significant trend in Egypt, because it may has been widely developed as a shear and drag fold direction during Jurassic-Cretaceous time as a result of the regional left lateral shear in the Tethyan region (Halsey 1975). This trend is considered to be the most profound fault trend which affects the Precambrian basement, and the more suitable lineaments in the overlying sediments in the Gulf of Suez and the Red Sea region (Abdel Gawad 1969). Dynamically, the N65°W trend is interpreted to be due to the shear couple that affected the Red Sea region (Meshref and El Sheikh 1973).

This Najd trend is characterized by being present on all frequency plots of all maps, similar to the Syrian arc or Qattara trend, so they could be considered as conjugate trends. Both trends gather up the characteristics of nearby trends. This means that, the Najd trend sums up the characteristics of both the Tethyan and Gulf of Suez-Red Sea trends, while the Syrian arc trend includes the characteristics of both the E-W and the Trans-African trends.

Tethyan or Mediterranean (E-W) trend

The characteristic features of the various peaks of this trend recorded in the various frequency plots are described briefly in Table 1.

According to the mechanical relations, and the hypothetical stress-strain ellipsoid, the fractures of this E-W trend could be interpreted to be due to a pressure with its principal stress axis being approximately N-S. Moreover, this trend might be rejuvenated later as one of the shear fractures parallel to one of the sides of the faulted blocks, that resulted from the assumed force of couple associated with the formation of the Red Sea (Ammar *et al.* 1983).

El Ghawaby 1979, mentioned that the axial trend of folds and the strike of thrust fault of the N-S directed stress pattern are expected to be E-W. Most geological maps of the Eastern Desert record the presence of such tight folding in many rock types (Sabet 1961, El Ghawaby 1973, Assaf 1973, Khawasik 1976). Also, the thrusting can be shown in many localities as the oldest rocks overthrust the lower horizons of Hammamat Sediments (Salman 1975, Ghanem 1968 and El Shazly and El-Ghawaby 1974). Both the folds axial trend and the strike of thrust faults are mostly deviated from the original E-W direction due to the effect of latter deformation.

The basement rocks West of the Nile are part of a regional NE-SW (in northern Sudan) to E-W (in Southern Egypt) striking fold belt which is bordered in the east with a conspicous tectonic contact by the Nubian shield. The major structural trends in this fold belt have been established during an Early to Middle Proterozoic compressive tectonic event which caused the regional trends of foliations and fold axes in the metamorphic basement (Schandelmeier *et al.* 1987).

El Gaby (1983) and Bernau *et al.* (1987) stated that in Southern Egypt, the major faults belong to a dextral 80° striking wrench fault system which is considered to be the conjugate shear system to the Najd fault system (Fig. 19). Youssef (1968) interpreted the E-W trend as an ancient fracture system that has been originated by compressive stresses acted mainly from N10°W and S10°E which were later slightly shifted westward. He also stated that the faults trending nearly E-W are not numerous, but most of them are major.

According to El Shazly (1966) the vertical stress exerted by the subsidence of the thick geosynclinal sediments led to the development of the major fracture lines of the E-W direction, along which the main geosynclinal volcanics are intruded.

This trend has been interpreted by Meshref (1980) to be due to the shift of African and South America, which initiated the northern compressive force affecting the rocks of North Africa.

From the present study, it could be stated that the E-W trend is interpreted as representing mainly folds and not faults. It is considered to be relatively ancient trend because it is represented only on the regional maps of the area and is lacking on the residual and basement tectonic maps.

Syrian arc or Qattara (ENE-WSW) trend

The characteristic features of the various peaks of this trend are described in Table 1.

The Syrian arc (or locally the Qattara) trend is the principal controlling direction

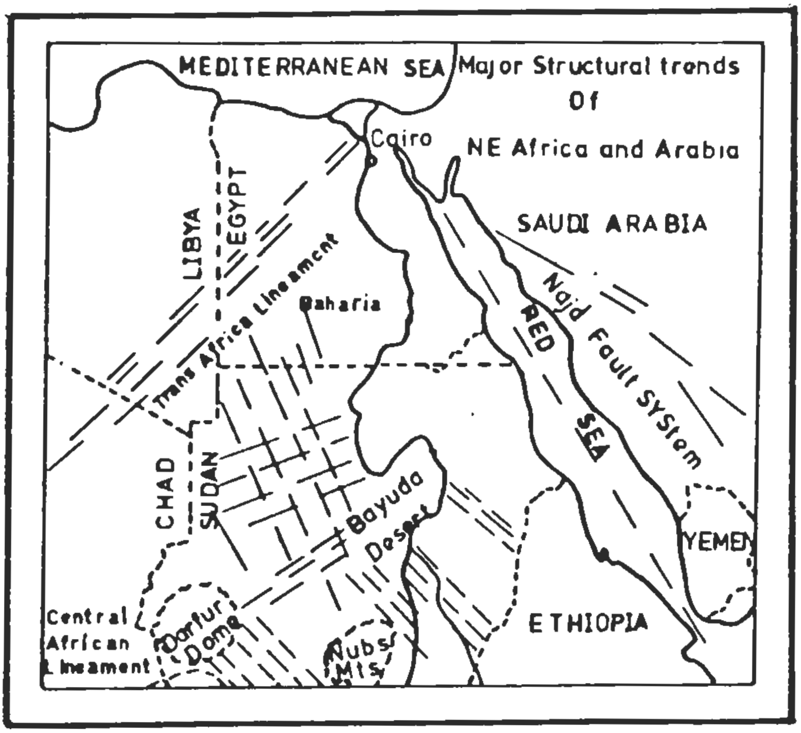

FIG. 19. Major shear and fracture zones of north-east Africa and Arabia at the end of Pan African consolidation (Schandelmeier *et al.* 1987).

of major folding in the unstable shelf region. It runs east-northeast across Egypt and is a predominant trend of the major axes of folds in northern Sinai. It may also be present as a trend of subsurface folding in the basement fault-block mosaic of the Gulf of Suez.

Youssef (1968), and Meshref and El Sheikh (1973) considered the Syrian arc trend to be the result of shifting of the northern horizontal pressure that resulted in the older E-W tectonic trend.

The Syrian arc-Qattara (ENE) trend is similar in all aspects to Najd (WNW) trend, since their peaks are recorded on all frequency plots interpreted from all maps.

Trans-African (NE-SW) trend

The characteristic features of peaks (representing the NE-SW trend) are described in Table 1.

This trend is recorded only by two peaks as interpreted from Fig. 8 and 12. This leads to the conclusion that it is not well-developed in this area of study.

El Shazly (1966) explained the NE-SW structural trends as transversal fractures to the major NW-SE fractures along which huge plutons were emplaced.

Meshref (1971) interpreted the NE-SW trend (with the NW-SE) to represent one of the two vertical shear fractures resulting from northern compression by the end of the mountain building stage and postorogenic transitional stage.

Garson and Krs (1976) considered the NE block faults in the Central and Southern Desert of Egypt may be partly due to vertical and partly due to transcurrent movements.

Ammar *et al.* (1983) mentioned that, the NE-SW trend was recorded over both the Precambrian basement rocks and the Phanerozoic cover sediments as revealed from the analysis of magnetic, radiometric and tectonic trends in the area. They added that, this trend however is more developed radiometrically and magnetically than tectonically. Therefore, they came to a conclusion that, the NE-SW trend could be considered valuable, as mineralization of economic importance either radioactive or magnetic or both could be connected with this system of fractures in the area.

The Meridional (N-S) and Aqaba (NNE-SSW) trends were found to be of minor importance as far as this area is considered. The peaks of both trends were recorded on the various frequency plots (especially the residual magnetic component and basement tectonic maps) under the line of critical frequency, and hence, they were considered statistically insignificant. Besides, they were not registered completely on regional magnetic component and the total gradient.

Structural Setting

Close examination of the two interpreted basement tectonic maps (Fig. 12 and 14) at the assigned interfaces (0.8 and 2.0 km) show the following features :

(1) The cental part of the study area is characterized by two major basement subsided blocks (or synclines) Nos. S1 and S2. The first one (S1) extends across the whole area of study from its southwestern corner to approximately its northeastern one, and trends in nearly an east northeast direction. The second one (S2) starts from the center of the area in a west northwest trend, then it changes to an east-west direction eastwards till the eastern edge of the area under investigation.

Mansour (1972) in his study of the Durunkat-Tarfawi area located in the east central portion of the area under consideration, identified a large basement syncline associated with the Shadli metavolcanics, occupying the central part of the study area. He mentioned also that this syncline extends for more than 25 kms in a WNW-ESE direction, while its maximum width approximates 5 kms. Its axis is identical with the elongated ridge of Gabal Abu Hamamid in Samiuki area; the average dip along both wings is relatively steep (50°-60°)

(2) To the north, another three major subsided basement blocks (or synclines) Nos. S3, S4 and S5, occupy the northern portion of the area under study. The first one (S3) from the west trends in a west northwest direction. The second (S4) lies in the extreme central northern part of the area and trends in nearly east-west direction changing to west northwest eastwards. The third one (S5) is situated in the northeastern part of the area and trends in a northwest direction. The three major subsided blocks (or synclines) S3, S4 and S5 seem to be continuous but were displaced by

major faults trending approximately in northwest changing to west northwest and northeast changing to east northeast directions.

(3) The five major subsided blocks (or synclines) are separated and bounded by five major uplifted blocks (or anticlines) either continuous or of the dissected (from A1 to A5). The axis of the first one (A1) is curved and occupies the southern portion of the study area. It shows a west northwest trend in its western part changed to an east notheast one in its eastern part.

(4) Between the two major subsided blocks (or synclines) S1 and S2, in the central eastern portion of the area under study, lies a major uplifted block (or anticline) A2, trending in an east-west direction. This part coincides with the location of Gabal Hamata elongated in the same manner.

(5) To the north of the major subsided block (or major syncline) S1, exist three major uplifted blocks (or major anticlines) A3, A4 and A5, all trending nearly in the same direction, east-west. These uplifted blocks seem to be dislocated (or displaced) by major faults trending approximately west northwest and east northeast.

Mansour (1972) stated that in the northern part of this area lie some granite masses forming the cores of large anticlines along Wadi Kharit, Wadi Naam and Wadi Hodein.

The results of statistical trend analysis of the interpreted axes of major uplifted and subsided blocks (anticlines and synclines) on the two basement tectonic maps at the two interfaces (0.8 and 2.0 km) have shown a number of peaks along the two frequency plots (Fig. 17a & b) centered at preferred values as evident from Table 2. In general, this analysis shows three major sets of folding at the following directions: Tethyan (E-W), Najd (WNW-ESE) and Syrian arc or Qattara (ENE-WSW) trends. These interpreted directions conform well with the work conducted by various authors in this field of geology in the Eastern Desert of Egypt, and surrounding areas.

The fault systems in the Southeastern Desert of Egypt include mainly two sets oriented NNW and ENE (Hunting 1967). The former being much more prominent. In some specific zones of the southeastern Desert of Egypt, the NNW faults are characterized by deep penetration into the earth's crust that may reach the upper mantle (Krs *et al.* 1973). They have great length of more than 100 kms, and a long history during which movement reoccurred. They probably were reactivated during the Caledonian and the Alpine Orogenies (Ivanov and Hussein 1972).

Statistical trend analysis of the faults interpreted from the two basement maps at the two interfaces (Fig. 12 and 14) of the Um Samiuki area has revealed that there is a strong relation between the magnetic trends and the tectonic history. From these analysis, it was possible to define the near-surface and deep-seated structural pattern in the area under study. Application of these modern geophysical techniques of interpretation to the observed magnetic data of this area of exposed (outcropping) basement rocks led to a satisfaction that the observed structural pattern on the surface are governed by the structural behaviour of the underlying deeply-buried crystaline rocks. This give a strong evidence for the active rejuvenation of the older structural trends that affected the area throughout the successive periods of its tectonic history.

The two frequency plots (Fig. 16 c & d) of the magnetic-tectonic lines at the two interfaces (0.8 and 2.0 km) and the two Tables (1 & 2) show a number of peaks above the line of critical (significant) frequency. These peaks could be grouped into four major sets of trends: the Gulf of Suez-Red Sea (NW-SE), the Najd (WNW-ESE), the Syrian arc or Qattara (ENE-WSW), and the Trans-African (NE-SW).

The NW-SE fault trend is associated with the deep-seated tectonic zones, especially in the western part of the area under consideration.

The WNW-ESE is considered to be the most profound fault trend which affects the Precambrian basement (Abdel Gawad 1969), and the ENE-WSW trends are represented by major faults crossing the whole area under study.

The NE-SW trend is met with only on the basement tectonic map at 0.8 km interface, and is represented by faults of limited extent.

The ring complex at Gabal El Kahfa in the southern part of this area is characterized by strong magnetic anomalies (Fig. 3).

Conclusion

Six modern geophysical techniques were applied to the interpretation of aeromagnetic survey data in South Eastern Desert of Egypt. These techniques include: the reduction to the north magnetic pole, the calculation of power spectrum for the determination of the two interfaces, the filtering combined with the analytical downward continuation, the normalized total vector (gradient), the calculation of total phase angle, and the statistical trend analysis using the overlap method. The outcome is ten interpretative maps and ten frequency plotes.

Interpretation of these various maps and plots provides a structural framework of the Um Samiuki area.

It was evident, from the application of the geophysical techniques, that this area is dissected by many faults having various trends and is constituted of many fold possessing different directions. The preferred major trends for the faults and folds are five and three in number respectively. These are: the Gulf of Suez-Red Sea (NW-SE and NNW-SSE), the Najd (WNW-ESE), Tethyan or Mediterranean (E-W), the Syrian arc or Qattara (ENE-WSW), and the Trans-African (NE-SW) trends. The Meridional (N-S), and the Aqaba (NNE-SSW) trends are represented in the area under study as a statistically insignificant directions.

The first-mentioned major trend is proved to be younger than the E-W trend, since it is recorded only on the near-surface maps. As far as the NNW-SSE trend, it proved to be of minor importance as far as this area is concerned. This trend is considered as a representative of major faulting in this area, but it is not interpreted as a representative of folding. It is associated with the deep-seated tectonic zones (diabase dykes) in the western part of the area from the original aeromagnetic data and in the central and east central parts of the area from the filtered magnetic data.

The Najd (WNW-ESE) and the Syrian arc or Qattara (ENE-WSW) trends are similar in all aspects, since their peaks were recorded on all frequency plots of all maps. They could be considered as conjugate trends, since they gather up the characteristics of the near-by trends. The first trend sums up the characteristics of both the Tethyan and the Gulf of Suez-Red Sea trends, while the second trend includes the characteristics of both the Tethyan and the Trans-African trends. Both trends correspond with two major sets of folding, which is confirmed from the work of various field geologists in Egypt and neighbouring areas.

The Tethyan or Mediterranean (E-W) trend could be interpreted as representing mainly folding rather than faulting, and is considered to be the most ancient trend, since it is represented only on the regional maps of this area.

The Trans-African (NE-SW) trend is not well-developed in the area under investigation, as a result of this study.

A characteristic magnetic features similar in many aspects to that recorded over Gabal El Kahfa ring complex and included within the same southern curved zone of magnetic highs was discovered from the filtered maps. Consequently, it could be concluded that it may represent another ring complex at depth, and therefore the eastern part of the area under study is deeper than its western one.

The Red Sea coast – in the area under consideration – is regarded as a major basement fault, since it separates two completely different magnetic characters on both sides.

Therefore, it could be concluded that the use of these modern geophysical techniques can lead to the delineation of the structural framework of the area, and they could be successfully applied in similar terrains of exposed Precambrian Basement rocks.

References

Abdel Gawad, A. (1969) New evidence of transcurrent movement in Red Sea area and petroleum implications, *Am. Assoc. Pet. Geol., Bull.* **33:** 1466-1479.

Aero-Service Report (1984b) *Final operational report of airborn magnetic/radiation survey in the Eastern Desert of Egypt for the Egyptian General Petroleum Corporation,* 6 vols. Aero-Service, Houston, Texas. April, 1984.

Affleck, J. (1963) Magentic anomaly trend and spacing patterns, *Geophysics* **28** (3): 379-395.

Akkad, M.K. and **El Ramly, M.F.** (1961) Geological history and classification of the Basement rocks of the Central Eastern Desert of Egypt, *Egypt. Geol. Surv. Miner. Res. Dept.* Paper **9,** 24 p.

Ammar, A.A., Meleik, M.L. and **Fouad, K.M.** (1983) Tectonic analysis of a sample area, Central Eastern Desert, Egypt, applying aeroradiometric and aeromagnetic survey data, *Bull. Fac. Earth Sci., King Abdulaziz University* **6:** 459-482.

Assaf, H.S. (1973) *Structure and radioactivity of Wadi Araqua area, Central Eastern Desert, Egypt.* Thesis, Ein Shams Univ., Cairo, Egypt (unpubl.).

Baranov, W. (1975) A new method for interpretation of aeromagnetic maps. Pseudogravimetric anomalies, *Geophysics* **22** (2): 121 p.

Bernau, R., Darbyshire, D.P.F., Fraz, G., Harms, U., Huth, A., Mansour, N., Pasteels, P. and **Schandelmeier, H.** (1987) Petrology, geochemistry and structural development of the Bir Safsaf-Aswan uplift/Southern Egypt. *J. Afr. Earth Sci.* **6** (1), pp. 79-90, Oxford.

Cianciara, B. and **Marcak, H.** (1976) Interpretation of gravity anomalies by means of local power spectrum, *Geophysical Prospecting* **24:** 273-286.

Cianciara, B. and **Marcak, H.** (1979) Geophysical anomaly interpretation of potential fields by means of singular points metbod and filtering, *Geophysical prospecting* **27:** 251-260.

El Gaby, S. (1983) Architecture of the Egyptian Basement Complex (Abstract). *5th Int. Conf. basement tectonics*, Cairo, October 16th-18th, pp. 19-20.

El Ghawaby, M.A. (1973) *Structure and radioactivity of Wadi Zeidun area, Central Eastern Desert, Egypt*, Ph.D. Thesis, Ein Shams Univ., Cairo, Egypt (unpubl.).

El Ghawaby, M.A. (1979) The tectonic development of north eastern corner of Africa. *Proceeding of the first geological congress of the Middle East GEOCOME-1; 4-7 Sept., Ankara, Turkey*, pp. 20-50.

El Shazly, E.M. (1964) On the classification of the Precambrian and other rocks of magmatic affiliation in Egypt. *Proc. XXII Int. Geo. Congr.*, Sec. **10,** pp. 88-101.

El Shazly, E.M. (1966) Structural development of Egypt, *Geol. Soc. Egypt, 4th Ann. Meet., Abstr.*, pp. 31-38.

El Shazly, E.M., Abdelhady, M.D., El Ghawahy, M.A. and **El Kassas, I.A.** (1974) Geologic interpretation of ERTS-1 Satellite Images for east Aswan area, Egypt. Proceedings, *Ninth Intern. Symp. on Remote Sensing of Environment*, Research Inst. of Michigan, Ann Arbor, Michigan, USA, pp. 104-117.

El Shazly, E.M. (1977) The geology of the Egyptian region, *In:* **Narin, A.E.M., Kanes, W.H.** and **Stehli, F.G. (Eds.)** The Ocean Basins and Margins, Plenum Publ. Corp., pp. 379-444.

El Shazly, E.M., Bakhit, F.S. and **Mostafa, M.E.** (1981) Significant structural trends and the relation to radioactivity in El Missikat granite pluton, Central Eastern Desert of Egypt. *Proceedings of the 6th Inter. Cong. for Stat., Comp. Sci. Soc. & Demogr. Res.*, Ein Shams Univ., Cairo, Egypt, **2,** pp. 399-417.

Farag, I.A.M. (1958) Stratigraphy of Egypt. Cairo University Press, Giza, 241 p.

Fouad, K.M., Ammar, A.A. and **Meleik, M.L.** (1987) Master curves for optimal reduction of total magnetic field data to the pole. *Proceedings of the 5th International Mathematical Geophysics Seminar held at the Free Univ. of Berlin, West Germany, pp. 125-135.*

Ghanem, M. (1968) *The geology of Wadi Kareim area, Eastern Desert, Egypt.* Thesis, Ph.D., Cairo Univ. (unpubl.).

Hall, D.H. (1964) Magnetic and tectonic recognition of Texada Island, British Columbia, *Geophysics* **29** (4): 566-581.

Halsey, J. (1975) Interpretation of ERTS linears, *Lecture Delivered for Egyptian Geologists in Cairo*, (unpubl.).

Harbough, J.W. and **Merriam, D.R.** (1968) *Computer application in stratigraphic analysis*, John Wiley and Sons, New York, London, Sydney.

Haugh, I., Brisbin, U.C. and **Turek, A.** (1967) A computer-oriented field sheet for structural data, *Can. J. Earth Sc.* **4:** 657-662.

Hunting Geology and Geophysics, Ltd. (1967) *Assessment of the Mineral Potential of the Aswan Region*, "Report", U.A.R.

Ivanove, T. and **Hussein, A.** (1972) A tectonic-geological report: *Assessment of the Mineral Potential of the Aswan Region, United Arab Republic.* Report for the United Nations Development Programme (UNDP), 137 p.

Johnson, L.N. and **Leone, C.R.** (1964) *Statistic and Experimental Design in Engineering and Physical Sciences*, John Wiley & Sons Inc., N.Y.

Khawasik, S.M. (1976) *Structural studies of El Atshan radioactive area Central Eastern Desert, Egypt*, Ph.D. Thesis, Cairo Univ., Cairo, Egypt (unpubl.).

Krs, M., Soliman, A.A. and **Amin, A.H.** (1973) Geophysical Phenomena over deep-seated tectonic zones in southern part of Eastern Desert of Egypt. *Annals Geol. Surv. Egypt* **2:** 125-138.

Lockwood Survey Corporation Ltd. (1968) Airborne magnetometer, Scientillation Counter, *Dual frequency electromagnetometer survey of part of the Aswan Region, United Arab Republic.* Report to the United Nation Development Programme, Toronto, Canada.

Mansour, M.S.M. (1972) *Geology of Drunkat-Tarfawi area, Sheikh Shadli Topographic sheet, South Eastern Desert, Egypt.* M.Sc. Thesis, Cairo University (unpubl.).

Meshref, W.M. (1971) The application of magnetic trend analysis to the interpretation of Egyptian tectonics, *Abstracts of papers presented at the 9th Annual Meeting of the Geological Society of Egypt*, pp. 19-21.

Meshref, W.M., Abdel Baki, S.H., Abdel Hady, H.M. and **Soliman, S.A.** (1980) Magnetic trend analysis in northern part of the Arabian-Nubian Shield and its tectonic implications. *Ann. Geol. Surv. Egypt* **10:** 939-953.

Qusa, M.E., Rashwan, A.A., Wasef, M.B., El Miligi, A.S., Aly, W.A., Khalil, M.A., Zahran, S.A., Hassan, O.A., Nasr, B.B., Mansour, M.M., Sadek, M.F., Salama, M.A. and **Khoteb, F.A.** (1978) *Geological map of Sheikh Shadli area, South Eastern Desert,* Geologic Survey of Egypt.

Riad, S. (1977) Shear zones in North Egypt interpreted from gravity data, *Geophysics* **42:** 1207-1214.

Sabet, A.H. (1961) *Geology and mineral deposits of Gebel El Sibai area, Red Sea Hills, Egypt, U.A.R.* Ph.D. Thesis, Leiden State Univ., The Netherlands, 168 p. (unpubl.).

Salman, A.B. (1975) *Structure and radioactivity of some phosphate deposits, East Luxur area, Egypt,* Ph.D. Thesis, Ein Shams Univ. (unpubl.).

Schandelmeier, H., Klitzsch, E., Hendriks, F. and **Wycisk, P.** (1987) *In:* **Eberh and Klitzsh** and **Eckant Schrank (eds.)** *Structural development of North-East Africa since Precambrian times,* Verlag Von Dietrich Reimer in Berlin, pp. 5-44.

Soliman, F., El Tahtawy, W. and **Fakhry, R.** (1978) *Internal report on the prospecting work carried out in Gabal Hamata area, South Eastern Desert,* Geological Survey of Egypt.

Spector, A. and **Grant, S.** (1970) Statistical models for interpreting aeromagnetic data, *Geophysics* **5:** 293-302.

Youssef, M.I. (1968) Structural pattern of Egypt and its interpretation. *Am. Assoc. Pet. Geol. Bull.* **52:** 601-614.

استخـدام التقنيات الجيوفيزيائية في تأويل معـطيات المسـاحة المغنطيسية الجوية ، جنوب الصحراء الشرقية ، مصر

أحمد أبو بكر عمار و سعيد إبراهيم ربيع

هيئة المواد النووية ، المعادي ، القاهــرة ، جمهورية مصر العربية

المستخلص . تم تخطيط البنية التركيبية الإقليمية لمنطقة ما تُدعى جبل أم سميوكي ، تقع جنـوب الصحراء الشرقية لمصر ، بوساطة تكامل ست تقنيات جيوفيزيائية حديثة ، من تأويلات معطيات المساحة المغنطيسية الجوية المحوَّلة إلى القطب الشمالي للأرض .

تم حساب سطحين بينيين متوسطين رئيسين على عمقي ٠,٨ ، و ٢ كيلو مترًا تحت مستوى القياس من خلال تطبيق طيف القدرة المحلي . تم تنفيذ ترشيح مُصاحَب باستمرار نازل تحليلي للمعـطيات المغنـطيسية الجـوية المحـوَّلة إلى القطب عند السطحيْن البينيين المحدَّدين . تم رسم أربع خرائط : اثنتين عند كل سطح بيني : إحداهما للمركبة الإقليمية والأخـرى للمـركبة المتبقية للمجال المغنطيسي . بالإضافة إلى ذلك ، تم حساب مقدار المتَّجـه (المَـيَّال) الكـلي العادي لشدة المجال عند السطحين المبيَّنين المعيَّنين ، وتم رسم خريطتين إضافيتين . علاوة على ما تقدَّم ، تم حساب تغيُّرات زاوية الطَّور ، وتم رسم خريطتين أخريتين . تم تطبيق تقنيات التحليل الإحصائي للوُجهات باستخدام طريقة التراكب لمعظم الخرائط الناتجة ، وتم رسم عشرة منحنيات تردد بيانيًا .

لقـد برهنت نتائج هذه الدراسة على وجود خمس وجهات مغنطيسية - تركيبية رئيسة تسمى : خليج السويس - البحر الأحمر (شمال شمال الغرب وشمال الغرب) ، نجد (غرب شمال الغرب) ، التيثي أو البحر المتوسط (شرق - غرب) ، القوس السُّوري أو القطارة (شرق شمال الشرق) ، وعبر إفريقيا (شمال الشرق) . لم يتم تسجيل وُجهتين في المنطقة تحت الـدراسـة ويُطلق عليهما : الزَّوالي (شمال - جنوب) ، وخليج العقبة (شمال شمال الشرق) . لقد وُجدَ أن الوجهات الأساسية المميَّزة لجميع أنماط الخطوط تتوافق إلى حد بعيد مع الاتجاهات الخمس المذكورة . هناك نُسق من الكتل الناتئة والمخسوفة (أو الطيَّات على هيئـة حَدَبات وقعائر) ترتبط جيدًا مع ثلاث وجهات رئيسة هي : غرب شمال الغرب ، شرق - غرب ، وشرق شمال الشرق . لقد ثبت تشابه وجهتي نجد والقوس السوري من عدة سمات ويمكن اعتبارهما وجهتين مترافقتين . تقترن النطاقات التشكيلية (التكتونية) المتغوِّرة (جُدَّات الديابيز) مع الوجهة الشمالية الغربية ، والتي يقع في أحدها مركب جبل الكهفة الحَلقي . لقد تم اكتشاف مَعلَم مماثل لجبل الكهفة على عمق ضمن نفس النطاق المغنطيسي مرتفع الشدة .